Accepted Manuscript

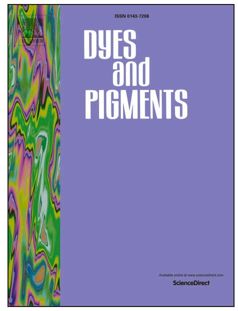

Synthesis, Optical Properties of Multi Donor-Acceptor Substituted AIE Pyridine Derivatives Dyes and Application for Au^{3+} Detection in Aqueous Solution

Junjuan Yang , Jiarong Li , Pengfei Hao , Fadong Qiu , Mingxing Liu , Qi Zhang , Daxin Shi

PII: S0143-7208(15)00008-X

DOI: 10.1016/j.dyepig.2015.01.005

Reference: DYPI 4632

To appear in: *Dyes and Pigments*

Received Date: 7 October 2014

Revised Date: 4 January 2015

Accepted Date: 6 January 2015

Please cite this article as: Yang J, Li J, Hao P, Qiu F, Liu M, Zhang Q, Shi D, Synthesis, Optical Properties of Multi Donor-Acceptor Substituted AIE Pyridine Derivatives Dyes and Application for Au^{3+} Detection in Aqueous Solution, Dyes and Pigments (2015), doi: 10.1016/j.dyepig.2015.01.005.

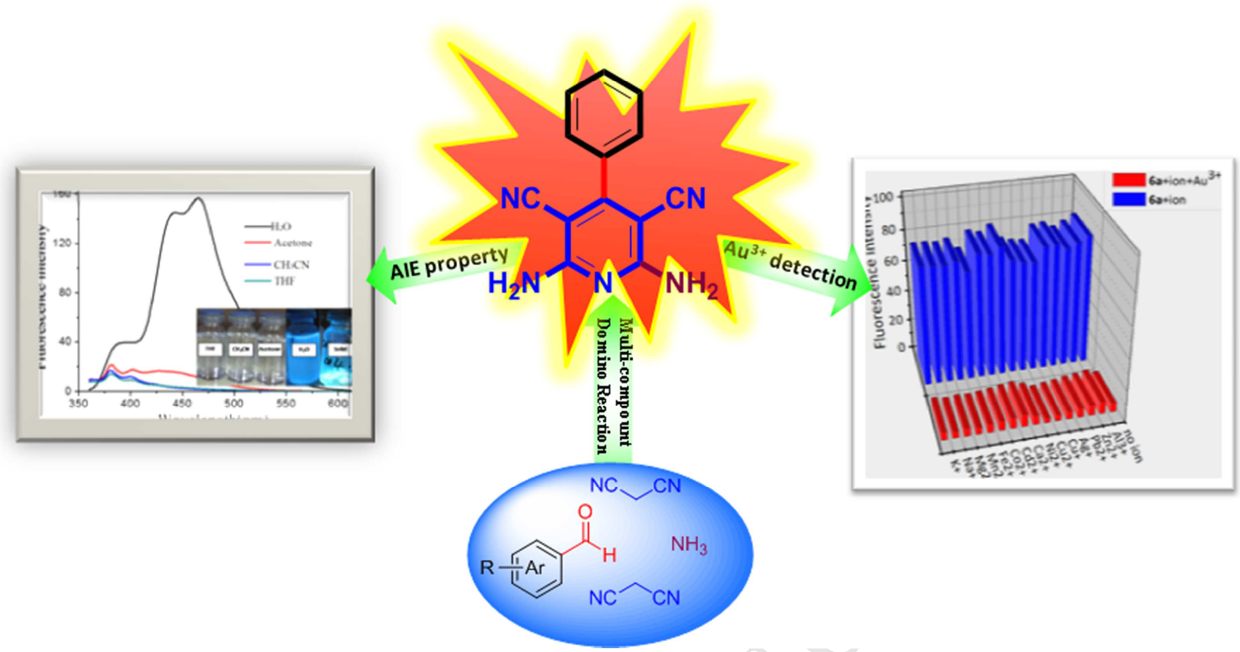
AIE property
Au3+ detection
Multi-component Domino Reaction
NC
CN
H2N
N
NH2
NH3
R
Ar
O
H
Acetone
THF
6a+ion+Au3+
6a+ion
Fluorescence intensity

Synthesis, Optical Properties of Multi Donor-Acceptor Substituted AIE Pyridine Derivatives Dyes and Application for Au^{3+} Detection in Aqueous Solution

Junjuan Yang, Jiarong Li, Pengfei Hao, Fadong Qiu, Mingxing Liu, Qi Zhang, and Daxin Shi*

School of Chemical Engineering and Environment, Beijing Institute of Technology, 100081 Beijing, China

*Corresponding author. Tel: (+86) 010/68918012 (S.D.X.); Fax (+86) 10-68918012 (S.D.X.)

E-mail address: shidaxin@bit.edu.cn

ABSTRACT: A series of multi donor-acceptor substituted pyridine derivative dyes were synthesed by three-component catalyst-free domino reaction in methanol aqueous at room temperature. The pyridine derivative dyes with thermally stable fluorescence exhibit aggregation-induced emission (AIE) in both aqueous solution and solid state due to the restricted intramolecular rotation as well. Furthermore, the family of molecule dyes showed nearly the full range of color emitters from blue to green and to orange. Moreover, the importance of dyes for heavy and transition metal ion species detection applications was demonstrated *via* the “turn off” detection of Au^{3+} in aqueous solution with the simple synthetic approach and high selectivity and sensitivity.

Keywords: Domino reaction, pyridine skeleton dyes, aggregation-induced emission, fluorescent probe, Au^{3+} detection

1. Introduction

Recently, photo-induced responsive organic luminescent dyes have been attracted much scientific and commercial attention [1]. Especially, they have been shown various applications, such as materials presenting semiconducting, fiber switcher, fluorescent sensor, and modulator [2]. In order to gain a long-lived organic dyes and to tune the electron-hole combination efficiency, the researchers have been devoted to the investigation of the multi donor-acceptor (D-A) systems such as D-A-D [3], A-D-A [4], and A-D-A-A [5]. In addition, aggregation-induced emission (AIE) dyes, as a kind of typical luminescent materials, were non-emissive in solution and highly fluorescent upon aggregate formation, which were contradicted to the expected aggregation caused quench (ACQ) effect of most traditional fluorophores [6]. Moreover, fluoregens bearing the AIE characteristic have been widely explored in bio-imaging, organic light-emitting diodes(OLEDs), as well as other fluorescent probes [7].

According to the green characteristics of atom economy, bond forming economy, and structural economy [8], new multi-component domino approaches for the synthesis of fluorescent compounds containing multi D-A groups have been a very interesting research topic [5, 9]. For example, Mukho-padhyay, *et al* synthesized A-D-A-A systems *via* a one-pot multi-component reaction catalyzed by zinc titanate nano-powder [5]; Gladow and co-workers reported a one-pot domino reaction to synthesize D-A systems of methylthio-substituted thiophene and pyrrole derivatives [9a].

4-aryl-2,6-diamino-3,5-dicyanopyridine derivatives **6** which exhibit π-conjugated flat rigid planar structure were a typical multi donor-acceptor (D-A-D-A-D) systems and were complied with structure characteristics of organic luminescent material dyes. Samadi, *et al* reported the synthesis of **6** by the amination of 2-amino-6-chloro-4-phenyl-3,5-dicyano pyridine [10] which was obtained from the condensation of malononitrile with triethyl orthobenzoate in the presence of pyridine [11]. And **6** were also obtained by the cyclization of arylidenemalononitrile, ethyl cyanoiminoacetate, and ammonium acetate in refluxing absolute ethanol (Scheme 1) [12]. However, these synthetic methods suffer from significant limitations such as low yield, toxic, and harsh reaction conditions.

To the best of our knowledge, a one-pot multi-component approach for the construction of this skeleton has not reported in the literature. Therefore, a more general, efficient, and viable route with operational simplicity for the synthesis of functionalized 2, 6-dicyanoanilines is highly desirable. Moreover, the optical properties of such systems were never investigated.

Owing to their simplicity, high sensitivity, and real-time detection, the construction of fluorescent probes for detecting heavy and transition metal ion species, have received a great deal of attentions [13]. Recently, several gold ion selective molecular sensors based on various fluorophore units including rhodamine [14], BODIPY [15], fluorescein [16], and naphthalimide [17] dyes have been reported. However, the most prominent drawback of those type of probes were the cross interferences with coexisting ions or only used in an organic or organic-containing solution. Moreover, some of the fluorescent probes sometimes suffer from intricate synthetic procedures.

Herein, we report on a rapid, efficient and convenient procedure for the synthesis of title dyes **6** *via* three component domino reaction in one pot (Scheme 2). These compounds showed AIE behaviour and can be used for gold ions detection in aqueous solution with high selectivity and sensitivity.

2. Results and discussion

2.1 Synthesis

In the initial experiment, we explored the optimum conditions for the synthesis of 4-aryl-2,6-diamino-3,5-dicyanopyridine derivatives **6** by the reaction of benzaldehyde **1a**, malononitrile **2** and ammonium hydroxide **4** as model substrate. The effects of different catalysts, solvents, and temperatures on the model reaction were examined and the results were listed in Table 1. Some available base such as NaOH, $NaOCH_3$, DBU, CH_3NH_2, $(C_2H_5)_3N$ can promote the reaction [18], and ammonia was the best, probably because of the relatively lower nucleophilicity

[8d]. Moreover, the excess ammonia was necessary (Table 1, entries 1-6). The reaction was performed in CH_2Cl_2, CH_3CN, THF, CH_3CH_2OH, CH_3OH, H_2O and methanol aqueous (Table 1, entries 7-12). Gratifyingly, we found that while the reaction was run in a mixture of methanol and water (volume ratio 6:1), the best result was obtained. These observations led to a conclusion that methanol aqueous is the solvent of choice, although a control experiment proved that water alone cannot promote the reaction (Table 1, entry 12) [19]. Additionally, methanol-water combination as solvent afforded a simple and clean purification of the products. The yields decreased when the temperature was higher than 40 ^{o}C, probably the more by-product was formed (Table 1, entries 13-16). Therefore, the optimal reaction condition was the reaction of benzaldehyde (**1a)** with 2.0 equivalents of malononitrile (**2**) and 2.0 equivalents ammonium hydroxide (**4**) at room temperature (25 ^{o}C) in methanol aqueous for 3.0 h and the yield of **6a** was 83% (Table 1, entry 13).

Furthermore, to demonstrate the scope and generality of this procedure for the synthesis of 2,6-diamino-3,5-dicyanopyridine **6**, a series of aromatic aldehydes **1a-o** were employed to react with **2** and **4** under the optimized conditions. As shown in Table 2, all the reactions underwent well to provide the desired 2,6-diamino-3,5-dicyanopyridines **6a-o** in good yields. Some fused aromatic aldehydes such as 3-pyridinecarbox-aldehyde, 1-naphthaldehyde, 9-anthraldehyde afforded the desired products **6b-6d** in 79-85% yields, respectively (Table 2, entries 2-4). To study the electronic and steric influences on the annulation strategy, a wide range of aldehydes **1** derived from benzene containing both electron-withdrawing and electron-donating groups in para, ortho or meta positon were employed and tolerated well (Table 2, entries 5-14). And steric hindrance as 2,6-disubstituted benzaldehyde also gave the desired product **6o** in 78% yield (Table 2, entry 15). Moreover, the structure of the domino reaction product **6c** was unambiguously confirmed by X-ray crystallography (Fig. 1).

In order to propose a suitable mechanism for the formation of **6**, a reaction between benzaldehyde **1a** and equimolar of malononitrile **2** in the presence of ammonium hydroxide **4** was allowed to stir for 30 min. The intermediate **3a** of Knoevenagel condensation was separated, and then **3a** reacted with equimolar of malononitrile **2** and ammonium hydroxide **4** in the optimal condition for 3.0 h to give the product **6a** in 81% yield. Hence we can conclude that the reaction proceeds through the formation of intermediate **3a** and a reasonable mechanistic pathway for one-pot three-component domino reaction is outlined in Scheme 3 and represented by the formation of **6a**. During the domino reaction process, the Knoevenagel condensation of one equivalent benzaldehyde **1a** with one equivalent malononitrile **2** was the initial step to form intermediate **3a** under the alkaline base condition [20]. Intermediate **3a** is supposed to undergo Michael addition with another equivalent malononitrile **2** under the catalysis of ammonia to furnish intermediate **5a** [21], followed by nucleophilic attacking of ammonia **4** on the cyano carbon of **5a**, to generate the cyclic intermediate **7a**. Intermediate **7a** was isomerized and dehydrated subsequently to provide the desired product **6a** [22].

2.2 Thermal stable properties

The thermal properties of selected **6a** and **6c** were gauged by both thermogravimetric analysis (TGA) and differential scanning calorimetry (DSC). Both of them exhibited high thermal stability as demonstrated by its TGA (Fig. 2), with its 5% weight loss temperature being up to 301.8 and 313.9 ℃. **6c** showed a higher melting temperature with a higher molecular weight. DSC analysis indicated that there were no phase transformation of **6a** and **6c** before the samples completely melted [23]. These results revealed that compounds **6** have excellent themally stable properties with the more potential applications in organic semiconductor or fluorescent sensor [24].

2.3 Optical properties

The optical properties of compounds **6** were examined by UV-vis and photoluminescence (PL) techniques in different solvent (Table 3). Interestingly, the compounds showed PL nearly in the full-color region from blue (**6a**) to green (**6l**) and to orange (**6m**) emitters by importing different groups such as OH, CN substituted on ortho position of phenyl scaffold. However, the correlation between optical properties and the molecular structures can currently be described only empirically. Compounds **6** showed the similar structure containing an aryl donor ring and a pyridine acceptor centres in a cross-shaped configuration (Fig. 1). In these multi D-A systems, the donor NH_2 groups and acceptor CN groups form dπ-nπ orbital overlap between pyridine center [23a, 25] and afford the π-conjugated interaction rigid planar structure which lead to the photoluminescence [26]. Furthermore, novel intermolecular interactions were noticed. As shown in Fig. 3, in the crystal of compound **6c**, there were a number of molecular pairs, and they pack in a parallel and face-to-face style. Each molecular pair was joined by hydrogen bonds and formed a dimer. Considering the special crystal structure and the relational fluorescent emissions in different solvent, it was reasonable to speculate that **6a** belong to the aggregation-induced emission (AIE) material [6a].

2.3.1 AIE properties of **6a**

We then examined photophysical properties of **6a**. As we can see from the inserts of Fig. 4, the non-solvent in H_2O solution and the separated solids of **6a** were strongly luminescent under the UV lamp (365 nm), while the good solvent solutions (in THF, CH_3CN, acetone) were not luminescent (Fig. 4). A solvent--nonsolvent photoluminescence was also studied. Compound **6a** was separately dispersed in THF (solvent)-water (nonsolvent) mixture systems, with the concentration being kept at 30 *u*M and *f*w stands for the water fraction. The photograph in Fig. 5a clearly shows the fluorescence enhancement of **6a** along with the increase of *f*w in THF/water mixture due to the poor solubility of **6a** in aqueous media. The photoluminescence intensity at nonsolvent (in H_2O) solution was about twenty times higher than in THF solvent. Unusual fluorescence amplification was also observed in both dilute and higher concentrations (Fig. 5c). The planar aromatic molecules with strong assembly properties exhibited amplified fluorescent sensing ability because of growing unidirectional π-π stacking and aggregation of the compound [9d]. The fluorescent emission of the **6a** was apparently induced by aggregation formation, and the compound was revealing an obvious AIE effect [6b, 7b, 27].

2.3.2 Mechanism of enhanced AIE

Many researchers have reported that the free rotations of such peripheral phenyl rings consume the excited state energy by nonradiative decay, thus quenching the emission in the solution [28]. In other words, energy loss of the excited state was related to structural flexibility. To gain insight the mechanism of enhanced AIE of **6a**, we changed structural flexibility by importing electron-donating group (compound **6l**) and electron-withdrawing group (compound **6m**) on ortho position of benzaldehyde **1** [29].

As shown in Fig. 6, compounds **6a**, **6l**, and **6m** exhibit characteristic absorptions at 300-520 nm in their electronic spectra corresponding to the π-π* transitions. And **6m** show an extraordinarily fluorescence peak between 400-550 nm. The large red shift in UV absorbance and fluorescence of **6l** and **6m** compared with that of **6a** were probably due to the hydrogen-bonding contacts of -OH and -CN which lead to the restricted rotation of the C-C single bonds between the aryl ring and the central pyridine plane [30]. In addition, -OH and -CN groups can form π-π stacking interactions between aryl ring with the pyridine plane and greatly improve the intramolecular rigidity [31].

Further support provided by the ^{1}H NMR titration experiments at various THF-water mixtures with different water fractions (*f*w) (Fig. S1), revealing that **6a** would undergo the aggregation process in aqueous media. Well-resolved proton signals with chemical shifts and splitting patterns consistent with the chemical formulation are observed in the THF solution and no proton signals observed in the D_2O solution due to the poor solubility of 6a in D_2O. With the increase of *f*w in aqueous mixture, the active hydrogen of amino group proton signal disappeared for the hydrogen exchange between D_2O and NH_2 group. Further increasing the water composition would result in a lower field shift and a splitting patterns of the signals corresponding to the phenyl group, suggestive of the presence of compound aggregation and π-π stacking in THF/water mixtures with different water fractions. For those reasons, it was reasonable to consider that the mechanism of enhanced AIE of **6a** was due to restricted intramolecular rotation (RIR) [32].

2.4 Application for detection of Au^{3+}

To investigate the potential application of **6a** for detecting metal ions, the responses of the fluorescence of **6a** probe solution (H_2O/DMSO, v:v, 100:1) toward Au^{3+}, Cu^{2+}, Al^{3+}, Zn^{2+}, Pb^{2+}, Ag^{+}, Cu^{+}, Ni^{2+}, Ca^{2+}, Cd^{2+}, Co^{2+}, Fe^{2+}, Mn^{2+}, Mg^{2+}, Na^{+}, and K^{+} aqueous solutions were studied (Fig. 7). The results showed that only Au^{3+} gave significant quenching effect on the fluorescence of **6a**, indicating the high selectivity of **6a** for the detection and specific recognition of Au^{3+} in aqueous solution. The effect of coexisting metal ions on the quenched fluorescence intensity of **6a** was performed which showed high anti-interference from other coexisting metal ions. These results indicated that **6a** could properly detect Au^{3+} ions in the mixtures of other species. To the best of our knowledge, this is the first reported example within the framework of AIE behavior whereby the addition of Au^{3+} “quenches” the fluorescent signal.

The flourescence response of probe **6a** in the aqueous solution toward various amounts of concentration Au^{3+} was examined. The flourescence intensity was measured immediately for each addition of Au^{3+} in the range from 0.3 uM to 100 uM. As shown in Fig. 8, the fluorescence intensity at 466 nm decrease rapidly with the lower concentration of Au^{3+} and reaches the saturation of intensity at about 1 equiv. Au^{3+} which reveals the possible formation of a 1:1 complex between **6a** and Au^{3+} [33]. This was further confirmed by the appearance of a peak at m/z 607.4 assignable to **6a**-Au^{3+} (**6a**+$AuCl_4^-$+$2H_2O$ complex) in the ESI-MS spectrum (Fig. S2) [34]. The quenching effect might be attributed to activate unsaturated bonds of CN of **6a** and form of complexes 1:1 between Au^{3+} and **6a** [14, 15]. Moreover, the quenching of 6**a** flourescence intensity shows a nearly linear curvature at relatively low Au^{3+} concentrations (0.3 ~ 4.0 μM, Fig. S3). The linear regression equation (c, μM) can be expressed as $1\text{-}I/Io = 0.094 + 0.089c$ for Au^{3+} with correlation coefficients (R^2) of 0.9946. The limit of detection is 0.3 uM for Au^{3+}. Therefore, compound **6a** could be used as a “turn-off” type fluorescent sensor in aqueous solution with the simple synthetic approach, high selectivity and sensitivity.

3. Conclusions

In conclusion, the novel approaches provide concise routes for the synthesis of some new fluorescent multi donor-acceptor pyridine derivatives in good yields by three-component catalyst-free domino reaction. A logical mechanism as well as a successful illation of a key intermediate was proposed. Furthermore, these pyridine derivatives showed nearly the full range of color emitters and AIE effect. Moreover, the compounds can be used as fluorescent probe for detection of Au^{3+} in aqueous solution with the simple synthetic approach and high selectivity and sensitivity.

4. Experimental section

4.1 Materials and Instrumentation

The solvent and all reagents were purchased from commercial sources and used without further purification. Water was deionized. The solutions of the metal ions were prepared from their chloride salts, except for Ag^+, which was $AgNO_3$. Melting points were determined using XT4 microscope melting pint apparatus (uncorrected). Infrared (IR) spectra were recorded on a Perkin Elmer FT-IR spectrophotometer with KBr-pellets. ^{1}H and ^{13}C NMR spectra were recorded at a Bruker 100, 400 or 500 MHz spectrometer with TMS as the internal standard. Mass spectra were recorded on a ZAB-HS mass spectrometer using ESI ionization. Elemental analyses were performed on an ElementarVario EL. The crystal structure was determined on a Bruker SMART 1000 CCD diffractometer. Ultraviolet-visible (UV) absorption were measured on a Hitachi U-3900H spectrophotometer using quartz cells of 1.0 cm path length (190-1100 nm scan range). Fluorescence spectra measurements were performed on a Hitachi F-7000 spectrofluorimeter with quartz cuvettes of 1.0 cm path length with a xenon lamp as the excitation source. TG and DSC were recorded on TG-DTA 6200 LAB SYS.

4.2 General procedure for the synthesis of multi donor-acceptor substituted pyridines derivatives

A solution of aldehyde (10 mmol), malononitrile (20 mmol) and 25% ammonium hydroxide (20 mmol) in the mixture of ethanol (60 mL) and water (10 mL) was stirred at proper temperature. After the reaction was completed as indicated by TLC, the precipitate of compounds **6** was collected by filtration. The crude product was recrystallization from 95% enthanol and THF solvent to provide the pure target products.

*4.3 Preparation of receptor **6a** solution*

6a was dissolved into THF solvent with a higher concentration of 10000 μM and then diluted to 10 μM by deionized water (18.5 MΩ) when used for measurements. The ration between THF and H_2O is 1:999 (v/v).

2-Benzylidenemalononitrile (3a): White solid; m.p. = 78-79 ^{o}C; IR (KBr, *v*, cm^{-1}): 3032, 2223, 1591, 1567, 1450, 1218, 957, 755; ^{1}H NMR (400 MHz, DMSO-*d6*) δ: 8.55 (s, 1H), 7.96-7.94 (m, 2H), 7.72-7.60 (m, 3H) ppm; ^{13}C NMR (100MHz, DMSO-*d6*), δ = 161.6, 134.4, 131.3 (2C), 130.5 (2C), 129.5, 114.2, 113.2, 81.6 ppm; MS (ESI): (*m/z*) = 155.1 ($[M+H]^+$, 100).

2,6-Diamino-4-phenylpyridine-3,5-dicarbonitrile (6a):[12] Yellow solid; m.p. > 300 °C; IR (KBr, *v*, cm^{-1}): 3475, 3425, 3363, 3220, 3158, 2205, 1674, 1624, 1586, 1558, 1540, 1458, 760; ^{1}H NMR (400 MHz, DMSO-*d6*) δ: 7.55-7.54 (m, 3H), 7.48-7.47 (m, 2H), 7.27 (s, 4H); ^{13}C NMR (100MHz, DMSO-*d6*), δ = 165 (2C), 161, 128.6 (3C), 128.3 (2C), 138, 116,5, 111,4, 79.8 (2C) ppm; MS (ESI): (*m/z*) = 236.0 ($[M+H]^+$, 100).

4,6-Diamino-2-(pyridin-3-yl)-3,5-dicarbonitrile (6b):[12] Green brown solid; m.p. > 300 °C; IR (KBr, *v*, cm^{-1}): 3408, 3333, 3177, 2202, 1651, 1582, 1530, 1486, 813; ^{1}H NMR (400 MHz, DMSO-*d6*) δ: 8.74-7.67 (m, 2H), 7.97-7.96 (m, 1H), 7.60-7.59 (m, 1H), 7.34 (s, 4H); ^{13}C NMR (100MHz, DMSO-*d6*), δ = 165.7, 161.1, 157.5, 151.2, 148.5, 136,4, 130,3, 123,6, 115.2, 114.8, 83.6, 83.4ppm; MS (ESI): (*m/z*) = 237.0 ($[M+H]^+$, 100).

2,6-Diamino-4-(naphthalen-1-yl)pyridine-3,5-dicarbonitrile (6c): White solid; m.p. > 300 °C; IR (KBr, *v*, cm^{-1}): 3262, 3062, 2929,1685, 1650, 1555, 1450, 1359, 1304, 1224, 990, 754; ^{1}H NMR (400 MHz, DMSO-d_6) *δ*: 8.10-8.05 (3H, m, Ar-H), 7.67-7.59 (m, 4H), 7.33 (s, 4H); ^{13}C NMR (100MHz, DMSO-d_6), δ = 160.8 (2C), 158.9, 133, 132.9, 129.6, 128.5 (2C), 127.2, 126.4, 126.2, 125.4, 124.3, 116.1 (2C), 81.3, 67.0 ppm; MS (ESI): (*m/z*) = 284.0 ($[M-H]^-$, 100); Anal. Calcd. for $C_{17}H_{11}N_5$: C, 71.57; H, 3.89; N, 24.55%. Found: C, 71.65; H, 3.92; N, 24.43%.

2,6-Diamino-4-(anthracen-9-yl)pyridine-3,5-dicarbonitrile (6d): Yellow solid; m.p. = 173-175 °C; IR (KBr, *v*, cm^{-1}): 3436, 2219, 1686, 1637, 1445, 1368, 1129, 1082, 903; ^{1}H NMR (400 MHz, $CDCl_3$) *δ*: 8.08-7.96 (4H, m, Ar-H), 7.61-7.52 (m, 4H), 4.13 (s, 4H); ^{13}C NMR (100MHz, $CDCl_3$), δ = 160.8(2C), 158.9, 133, 132.9, 129.6(2C), 128.5(2C), 127.2, 126.4, 126.2 (2C), 125.4 (2C), 124.3 (2C), 116.1 (2C), 81.3 (2C) ppm; MS (ESI): (*m/z*) = 334.0 ($[M-H]^-$, 100); Anal. Calcd. for $C_{21}H_{13}N_5$: 75.21; H, 3.91; N, 20.88%. Found: C, 75.38; H, 3.87; N, 20.79%.

2,6-Diamino-4-(4-chlorophenyl)pyridine-3,5-dicarbonitrile (6e):[12] White solid; m.p. >300 ^{o}C; IR (KBr, *v*, cm^{-1}): 3478, 3419, 3364, 3173, 2209, 1622, 1573, 1558, 1541, 1453, 1313, 1035, 764; ^{1}H NMR (400 MHz, DMSO-d_6) δ: 7.65 (m, 1H), 7.55-7.47 (m, 3H), 7.35 (m, 4H); ^{13}C NMR (100MHz, DMSO-d_6), δ = 165 (2C), 160, 138.9, 132.1, 131.4, 130.1, 129.72, 127.7, 115.7 (2C), 80.4 (2C) ppm; MS (ESI): (*m/z)* = 268.1([M-H]$^-$, 100).

2,6-Diamino-4-(fluorophenyl)pyridine-3,5-dicarbonitrile (6f): Gry solid; m.p. >300 ^{o}C; IR (KBr, *v*, cm^{-1}): 3480, 3424, 3367, 2204, 1624, 1569, 1515, 1453, 1245, 844; ^{1}H NMR (400 MHz, DMSO-d_6) δ: 7.57-7.53 (m, 2H), 7.36-7.40 (m, 2H), 7.28 (m, 4H); ^{13}C NMR (100MHz, DMSO-d_6), δ = 163.2 (2C), 163.0, 160.9, 130.7, 130.9 (2C), 116.4, 115.7, 115.5 (2C), 79.9, 77.62 ppm; MS (ESI): (*m/z)* = 254.3([M+H]$^+$, 100); Anal. Calcd. for $C_{13}H_8FN_5$: C, 61.66; H, 3.18; N, 27.66%. Found: C, 61.75; H, 3.13; N, 27.68%.

2,6-Diamino-4-(4-methoxyphenyl)pyridine-3,5-dicarbonitrile (6g): White solid; m.p. >300 ^{o}C; IR (KBr, *v*, cm^{-1}): 3480, 3435, 3370, 3155, 2205, 1674, 1627, 1582, 1519, 1268, 1176, 1020, 841; ^{1}H NMR (400 MHz, DMSO-d_6) δ: 7.44-7.42 (m, 2H), 7.21 (s, 4H), 7.09-7.07 (m, 2H), 3.83 (s, 3H); ^{13}C NMR (500MHz, DMSO-d_6), δ = 161.6 (2C), 160.9, 159.9, 130.4, 127.5 (2C), 117.2 (2C), 114.4 (2C), 80.2 (2C), 55.8 ppm; MS (ESI): (*m/z)* = 264.1 ([M-H]$^-$, 100); Anal. Calcd. for $C_{14}H_{11}N_5O$: C, 63.39; H, 4.18; N, 26.40%. Found: 63.48; H, 4.19; N, 26.30%.

2,6-Diamino-4-(4-hydroxyphenyl)pyridine-3,5-dicarbonitrile (6h): White solid; m.p. >300 ^{o}C; IR (KBr, *v*, cm^{-1}): 3416, 3368, 3166, 2205, 1626, 1565, 1539, 1302, 1173, 841; ^{1}H NMR (400 MHz, DMSO-d_6) δ: 9.97 (s, 1H), 7.33-7.30 (m, 2H), 7.19 (m, 4H), 6.90-6.88 (m, 2H); ^{13}C NMR (500MHz, DMSO-d_6), δ = 161.6 (2C), 160.2, 159.4, 130.4, 125.9 (2C), 117.3 (2C), 115.7 (2C), 80.1 (2C) ppm; MS (ESI): (*m/z)* = 250.1 ([M-H]$^-$, 100); Anal. Calcd. for $C_{13}H_9N_5O$: C, 62.15; H, 3.61; N, 27.87%. Found: 62.21; H, 3.62; N, 27.78%.

2,6-Diamino-4-(2-chlorophenyl)pyridine-3,5-dicarbonitrile (6i): White solid; m.p.>300 ^{o}C; IR (KBr, *v*, cm^{-1}): 3365, 2209, 1662, 1624, 1577, 1553, 1539, 1494, 1316, 1094, 835; ^{1}H NMR (400 MHz, DMSO-d_6) δ: 7.63-7.61 (m, 2H), 7.53-7.51 (m, 2H), 7.31 (m, 4H); ^{13}C NMR (500MHz, DMSO-d_6), δ= 161.4 (2C), 159.1, 135.2, 134.4, 130.8 (2C), 129.2 (2C), 116.8 (2C), 80.2 (2C) ppm; MS (ESI): *(m/z)* = 268.1([M-H]$^{-}$, 100); Anal. Calcd. for $C_{13}H_8ClN_5$: 57.90; H, 2.99; N, 25.97%. Found: C, 57.80; H, 3.02; N, 25.83%.

2,6-Diamino-4-(2-ethoxyphenyl)pyridine-3,5-dicarbonitrile (6j): White solid; m.p. >300 ^{o}C; IR (KBr, *v*, cm^{-1}): 3497, 3455, 3344, 3228, 2208, 1640, 1619, 1562, 1540, 1449, 1227, 765; ^{1}H NMR (400 MHz, DMSO-d_6) δ: 7.48-7.46 (m, 2H), 7.40-7.26, (m, 1H), 7.20 (m, 4H), 7.07-7.04 (m, 1H), 4.12-3.97(q, 3H, J = 60.8), 1.29-1.26 (t, 2H, J = 13.6); ^{13}C NMR (500MHz, DMSO-d_6), δ = 161.3 (2C), 158.1, 155.6, 131.7, 130.2 (2C), 124.6, 120.9, 116.8, 113.3 (2C), 81.3 (2C), 64.2, 14.9 ppm; MS (ESI): *(m/z)* = 278.3([M-H]$^{-}$, 100); Anal. Calcd. for $C_{15}H_{13}N_5O$: 64.51; H, 4.69; N, 25.07%. Found: 64.59; H, 4.71; N, 24.96%.

2,6-Diamino-4-(3-nitrophenyl)pyridine-3,5-dicarbonitrile (6k): White solid; m.p. >300 ^{o}C; IR (KBr, *v*, cm^{-1}): 3451, 3350, 3226, 2211, 1644, 1562, 1530, 1353, 1168; ^{1}H NMR (100 MHz, DMSO-d_6) δ: 8.42-8.40 (s, 1H), 7.98 (m, 1H), 7.86 (m, 2H), 7.38 (s, 4H); ^{13}C NMR (500MHz, DMSO-d_6), δ = 161.3 (2C), 157.9, 148.1, 137.1, 135.6, 131.0, 125.2, 123.8, 116.7 (2C), 80.3 (2C) ppm; MS (ESI): *(m/z)* = 279.2 ([M-H]$^{-}$, 100); Anal. Calcd. for $C_{13}H_8N_6O_2$: C, 54.34; H, 2.47; N, 24.21%. Found: C, 54.43; H, 2.48; N, 24.19%.

2,6-Diamino-4-(2-hydroxyphenyl)pyridine-3,5-dicarbonitrile (6l): White solid; m.p. 223-225 ^{o}C; IR (KBr, *v*, cm^{-1}): 3345, 3132, 2210, 1647, 1608, 1559, 1541, 1477, 764; ^{1}H NMR (400 MHz, $CDCl_3$) δ: 9.08-9.05 (s, 1H), 7.54-7.51 (m, 3H), 7.16-7.13(m, 1H), 4.05 (s, 4H); ^{13}C NMR (100MHz, DMSO-d_6), δ = 166.7, 159.9, 154.8, 151.8, 133.5, 125.2, 123.6, 117.6, 116.6, 115.5 (2C), 75.4, 71.8 ppm; MS (ESI): *(m/z)* = 273.1([M+Na]$^+$, 100); Anal. Calcd. for $C_{13}H_9N_5O$: 62.15; H, 3.61; N, 27.87%. Found: C, 62.25; H, 3.61; N, 27.76%.

2,6-Diamino-4-(2-cyanophenyl)pyridine-3,5-dicarbonitrile (6m): Reddish brown solid; m.p. >300 ^{o}C; IR (KBr, *v*, cm^{-1}): 3548, 3476, 3412, 2208, 2204, 1637, 1618, 1490, 1384, 1111; ^{1}H NMR (400 MHz, DMSO-d_6) δ: 7.65 (m, 1H), 7.56-7.46(m, 3H), 7.35 (s, 4H); ^{13}C NMR (100MHz, DMSO-d_6), δ = 166.1, 161.5, 158.8, 148.1, 136.1, 135.6, 131.6, 125.6, 123.9, 117.1, 115.7, 115.3, 84.0, 83.9 ppm; MS (ESI): *(m/z)* = 259.3 ([M-H]$^-$, 100); Anal. Calcd. for $C_{14}H_8N_6$: C, 64.61; H, 3.10; N, 32.29%. Found: C, 64.74; H, 3.15; N, 32.17%.

2,6-Diamino-4-(2,4-dichlorophenyl)pyridine-3,5-dicarbonitrile (6n): White solid; m.p. 226-228 ^{o}C; IR (KBr, *v*, cm^{-1}): 3468, 3331, 3226, 2218, 1634, 1576, 1547, 1367, 997; ^{1}H NMR (500 MHz, $CDCl_3$) δ: 7.61 (s, 1H), 7.45-7.43 (m, 1H), 7.29 (m, 1H), 4.08 (s, 4H); ^{13}C NMR (100MHz, DMSO-d_6), δ = 163.7 (2C), 160.5, 137.2, 135.8, 131.6, 129.5, 128.2, 122.6, 115.9, 114,6, 80.3, 79.9 ppm; MS (ESI): *(m/z)* = 305.1([M+H]$^+$); Anal. Calcd. for $C_{13}H_7Cl_2N_5$: 51.34; H, 2.32; N, 23.03%. Found: C, 51.38; H, 2.27; N, 23.13%.

2,6-Diamino-4-(2-chloro-6-fluorophenyl)pyridine-3,5-dicarbonitrile (6o): White solid; m.p. >300 ^{o}C; IR (KBr, *v*, cm^{-1}):3480, 3428, 3356, 3181, 2211, 1666, 1625, 1574, 1445, 1314, 1248, 909, 792; ^{1}H NMR (400 MHz, DMSO-d_6) δ: 7.67-7.51 (m, 3H), 7.47 (m, 4H); ^{13}C NMR (500MHz, DMSO-d_6), δ = 161.2 (2C), 160.1, 158.1, 133.4, 132.9, 126.5, 122.9, 115.8, 115.7, 115.5, 80.9 (2C) ppm; MS (ESI): *(m/z)* = 286.0([M-H]$^-$, 100); Anal. Calcd. for $C_{13}H_7ClFN_5$: C, 54.28; H, 2.45; N, 24.34%. Found: C, 54.34; H, 2.47; N, 24.21%.

Appendix A. Supplementary material

Crystallographic data (excluding structure factors) for the structure in this paper have been deposited with the Cambridge Crystallographic Data Centre as supplementary publication no.

CCDC 1018482. Copies of the data can be obtained free of charge on application to CCDC, 12 Union Road, Cambridge CB2 1EZ, UK, (fax: +44 (0)1223 336033 or e-mail: deposit@ccdc.cam.ac.uk).

Appendix B. Supplementary dat

Supplementary data related to this article can be found at http://dx.doi.org/10.1016/j.dyepig.******.

Acknowledgement

This work was supported by the grant of Beijing Institute of Technology. We are grateful for analytical help of Institute of Chemistry, Chinese Academy of Sciences and Beijing Normal University.

References

[1] (a) Li JY, Zhang T, Liang YJ, Yang RX. Solution-processible carbazole dendrimers as host materials for highly efficient phosphorescent organic light-emitting diodes. Adv Funct Mater 2013; 23: 619-28; (b) Llanes-Pallas A, Yoosaf K, Traboulsi H, Mohanraj J, Seldrum T, Dumont J, et al. Modular engineering of H-bonded supramolecular polymers for reversible functionalization of carbon nanotubes. J Am Chem Soc 2011; 133:15412-24; (c) Li TY, Liang X, Wu C, Xue LS, Xu QL, Zhang S, et al. Syntheses crystal structure photophysical property and theoretical study of a new series of iridium complexes with *N*-(diphenyl- phosphoryl)benzamide derivatives as the ancillary ligands. J. Organomet. Chem. 2014;755: 110-9; (d) Lee CW, Lee JY. High quantum efficiency and color stability in white phosphorescent organic light emitting diodes using a pyridine modified carbazole derivative. Dyes Pigments 2014; 103: 34-8.

[2] (a) Kwon SM, Yoon JY, Lee KH, Kim BY, Lee SJ, Kim YK, et al. Blue organic light-emitting

diodes based on new bipolar anthracene derivatives containing pyridine. J Nanosci Nanotechnol 2014; 14: 6116-9; (b) Fang JM, Selvi S, Liao JH, Slanina Z, Chen CT, Chou PT. Fluorescent and circular dichroic detection of monosaccharides by molecular sensors: bis[(pyrrolyl)ethynyl] naphthyridine and bis[(indolyl)ethynyl] naphthyridine. J Am Chem Soc 2004; 126: 3559-66; (c) Winkler M, Houk K. Nitrogen-rich oligoacenes: candidates for *n*-channel organic semiconductors. J Am Chem Soc 2007;129: 1805-15.

[3] (a) González M, Segura JL, Seoane C, Martín N, Garín J, Orduna J, et al. Tetrathiafulvalene derivatives as NLO-phores: Synthesis electrochemistry raman spectroscopy theoretical calculations and NLO properties of novel TTF-derived donor-π-acceptor dyads. J Org Chem 2001; 66: 8872-82; (b) Andersson AS, Diederich F, Nielsen MB. Acetylenic tetrathia-fulvalene-dicyanovinyl donor-acceptor chromophores. Org Biomol Chem 2009; 7: 3474-80.

[4] Cui SL, Lin XF, Wang YG. Parallel synthesis of strongly fluorescent polysubstituted 2,6-dicyanoanilines *via* microwave-promoted multicomponent reaction. J Org Chem 2005; 70: 2866-9.

[5] Das P, Butcher RJ, Mukhopadhyay C. Zinc titanate nanopowder: an advanced nanotechnology based recyclable heterogeneous catalyst for the one-pot selective synthesis of self-aggregated low-molecular mass acceptor-donor- acceptor-acceptor systems and acceptor-donor-acceptor triads. Green Chem 2012; 14: 1376-87.

[6] (a) Hu R, Leung NLC, Tang BZ. AIE macromolecules: syntheses structures and functionalities. Chem Soc Rev 2014; 43: 4494-562; (b) Chen Y, Li M, Hong Y, Lam JWY, Zheng Q, Tang BZ. Dual-modal MRI contrast agent with aggregation-induced emission characteristic for liver specific imaging with long circulation lifetime. ACS Appl Mater Interfaces 2014; 6: 10783-91; (c) Liu Y, Tao X, Wang F, Dang X, Zou D, Ren Y, et al. Aggregation-induced emissions of

fluorenonearylamine derivatives: a new kind of materials for nondoped red organic light-emitting diodes. J Phys Chem C 2008; 112: 3975-81; (d) Liu Y, Tao X, Wang F, Shi J, Sun J, Yu W, et al. Intermolecular hydrogen bonds induce highly emissive excimers: enhancement of solid-state luminescence. J Phys Chem C 2007; 111: 6544-49.

[7] (a) Gao M, Sim CK, Leung CWT, Hu Q, Feng G, Xu F, et al. A fluorescent light-up probe with AIE characteristics for specific mitochondrial imaging to identify differentiating brown adipose cells. Chem Commun 2014; 50: 8312-5; (b) Gao M, Hu Q, Feng G, Tang BZ, Liu B. A fluorescent light-up probe with "AIE + ESIPT" characteristics for specific detection of lysosomal esterase. J Mater Chem B 2014; 2: 3438-42; (c) Anariba F, Chng LL, Abdullah NS, Tay FEH. Syntheses optical properties and bioapplications of the aggregation-induced emission of 2,3,4,5-tetraphenylcyclopenta-2,4-dienyl benzene derivatives. J Mater Chem 2012; 22: 19303-10.

[8] (a) Kumaravel K, Vasuki G. Four-component catalyst-free reaction in water: Combinatorial library synthesis of novel 2-amino-4-(5-hydroxy-3-methyl-1*H*-pyrazol-4-yl)-4*H*-chromene-3-carbonitrile derivatives. Green Chem 2009; 11: 1945-7; (b) Kolb HC, Finn MG, Sharpless KB. Click chemistry: Diverse chemical function from a few good reactions. Angew Chem Int Edit 2001; 40: 2004-9; (c) Tietze LF. Domino reactions in organic synthesis. Chem. Rev. 1996; 96: 115-36; (d) Janvier P, Sun XW, Bienayme H, Zhu JP. Ammonium chloride-promoted four-component synthesis of pyrrolo 3,4-b pyridin-5-one. J Am Chem Soc 2002; 124: 2560-7; (e) Volla CMR, Atodiresei L, Rueping M. Catalytic C-C Bond-forming multi-component cascade or domino reactions: pushing the boundaries of complexity in asymmetric organo-catalysis. Chem. Rev. 2014; 114: 2390-431; (f) Banfi L, Basso A, Moni L, Riva R. The alternative route to enantiopure multicomponent reaction products: biocatalytic or organo-

catalytic enantioselective production of inputs for multicomponent reactions. Eur J Org Chem 2014; 2014: 2005-15.

[9] (a) Gladow D, Reissig HU. Perfluoroalkyl-substituted thiophenes and pyrroles from donor-acceptor cyclopropanes and heterocumulenes: synthesis and exploration of their reactivity. J Org Chem 2014; 79: 4492-502; (b) Dengiz C, Dumele O, Kato SI, Zalibera M, Cias P, Schweizer WB, et al. From homoconjugated push-pull chromophores to donor-acceptor-substituted spiro systems by thermal rearrangement. Chem Eur J 2014; 20: 1279-86; (c) Mu X, Qi L, Qiao J, Ma H. One-pot synthesis of tyrosine-stabilized fluorescent gold nanoclusters and their application as turn-on sensors for Al^{3+} ions and turn-off sensors for Fe^{3+} ions. Analytical Methods 2014; 6: 6445-51; (d) Zonouzi A, Hosseinzadeh F, Karimi N, Mirzazadeh R, Ng SW. Novel approaches for the synthesis of a library of fluorescent chromenopyrimidine derivatives. ACS Combinatorial Science 2013; 15: 240-6.

[10] Samadi A, Silva D, Chioua M, do Carmo Carreiras M, Marco Contelles J. Microwave irradiation-assisted amination of 2-chloropyridine derivatives with amide solvents. Synthetic Commun 2011; 41: 2859-69.

[11] (a) Schmidt H. W, Junek H. Zur Synthese von Alkoxymethylenmalonitrilen tetracyano-propeniden und hochsubstituierten *α*-Aminopyridinen. Monatshefte für Chemie 1977; 108: 895-900; (b) Piper J, McCaleb G, Montgomery J, Kisliuk R, Gaumont Y, Sirotnak F. Syntheses and antifolate activity of 5-methyl-5-deaza analogs of aminopterin methotrexate folic acid and N10-methylfolic acid. J Med Chem 1986; 29: 1080-7.

[12] Mashaly M, Hammouda M. New simple and one-pot synthetic routes to polyfunctionally substituted pyridines; 1,4-dihydropyridazines and 4*H*-1,2-oxazine. Zeitschrift Fur Natur-forschung B 1999; 54: 1205-9.

[13] (a) Charier S, Ruel O, Baudin JB, Alcor D, Allemand JF, Meglio A, et al. An efficient fluorescent probe for ratiometric pH measurements in aqueous solutions. Angew Chem Int Ed Engl 2004; 43: 4785-8; (b) Goswami S, Sen D, Das NK. A new highly selective ratiometric and colorimetric fluorescence sensor for Cu^{2+} with a remarkable red shift in absorption and emission spectra based on internal charge transfer. Org Lett 2010; 12: 856-9; (c) Wang JB, Qian XH. A series of polyamide receptor based PET fluorescent sensor molecules: Positively cooperative Hg^{2+} ion binding with high sensitivity. Org Lett 2006; 8: 3721-4; (d) Shi W, Ma FD, Hui YH, Mi HY, Tian Y, Lei YL, et al. TCNE-decorated triphenylamine-based conjugated polymer: Click synthesis and efficient turn-on fluorescent probing for Hg^{2+}. Dyes Pigments 2014; 104: 1-7; (e) Huang JG, Tang M, Liu M, Zhou M, Liu Z. G, Cao Y, et al. Development of a fast responsive and highly sensitive fluorescent probe for Cu^{2+} ion and imaging in living cells. Dyes Pigments 2014; 107: 1-8.

[14] (a) Yang YK, Lee S, Tae J. A Gold(III) ion-selective fluorescent probe and its application to bioimagings. Org Lett 2009; 11: 5610-3; (b) Karakus E, Ucuncu M, Emrullahoglu M. A rhodamine/BODIPY-based fluorescent probe for the differential detection of Hg(II) and Au(III). Chem Commun 2014; 50: 1119-21.

[15] (a) Ucuncu M, Emrullahoglu M. A BODIPY-based reactive probe for the detection of Au(III) species and its application to cell imaging. Chem Commun 2014; 50: 5884-6; (b) Wang JB, Wu QQ, Min YZ, Liu YZ, Song QH. A novel fluorescent probe for Au(III)/Au(I) ions based on an intramolecular hydroamination of a Bodipy derivative and its application to bioimaging. Chem Commun 2012; 48: 744-6; (c) Park J, Choi S, Kim T. I, Kim Y. Highly selective fluorescence turn-on sensing of gold ions by a nanoparticle generation/C-I bond cleavage sequence. Analyst 2012; 137: 4411-4.

[16] Patil NT, Shinde VS, Thakare MS, Hemant Kumar P, Bangal PR, Barui AK, et al. Exploiting the higher alkynophilicity of Au-species: development of a highly selective fluorescent probe for gold ions. Chem Commun 2012; 48: 11229-31.

[17] Choi JY, Kim GH, Guo Z, Lee HY, Swamy KM, Pai J, et al. Highly selective ratiometric fluorescent probe for Au^{3+} and its application to bioimaging. Biosens Bioelectron 2013; 49: 438-41.

[18] (a) Xue D, Mu Y, Mao Y, Yang T, Xiu Z. Kinetics of DBU-catalyzed transesterification for biodiesel in the DBU-ethanol switchable-polarity solvent. Green Chem 2014; 16: 3218-23; (b) Coady DJ, Fukushima K, Horn H. W, Rice JE, Hedrick JL. Catalytic insights into acid/base conjugates: highly selective bifunctional catalysts for the ring-opening polymerization of lactide. Chem Commun 2011; 47: 3105-7; (c) Tanabe Y, Misaki T, Kurihara M, Iida A, Nishii Y. Silazanes/catalytic bases: mild powerful and chemoselective agents for the preparation of enol silyl ethers from ketones and aldehydes. Chem Commun 2002; 15: 1628-9.

[19] (a) Prasanna P, Perumal S, Menéndez JC. Chemodivergent multicomponent domino reactions in aqueous media: l-proline-catalyzed assembly of densely functionalized 4*H*-pyrano[2,3-c]pyrazoles and bispyrazolyl propanoates from simple acyclic starting materials. Green Chem 2013; 15: 1292-9; (b) Khalafi-Nezhad A, Sarikhani S, Shahidzadeh ES, Panahi F. l-Proline-promoted three-component reaction of anilines aldehydes and barbituric acids/malononitrile: regioselective synthesis of 5-arylpyrimido[45-b]quinoline-diones and 2-amino-4-aryl-quino-line-3-carbonitriles in water. Green Chem 2012; 14: 2876-84.

[20] (a) Liang F, Cheng X, Liu J, Liu Q. Efficient three-component one-pot synthesis of fully substituted pyridin-2(1*H*)-ones via tandem Knoevenagel condensation-ring-opening of cyclopropane-intramolecular cyclization. Chem Commun 2009; 24: 3636-8; (b) Thakur A,

Tripathi M, Rajesh UC, Rawat DS. Ethylene- diammonium diformate (EDDF) in PEG600: an efficient ambiphilic novel catalytic system for the one-pot synthesis of 4*H*-pyrans via Knoevenagel condensation. RSC Adv 2013; 3: 18142-8; (c) Li G, Xiao J, Zhang W. Knoevenagel condensation catalyzed by a tertiary-amine functionalized polyacrylonitrile fiber. Green Chem 2011; 13: 1828-36; (d) Dong X, Hui Y, Xie S, Zhang P, Zhou G, Xie Z. Schiff base supported MCM-41 catalyzed the Knoevenagel condensation in water. RSC Adv 2013; 3: 3222-6.

[21] (a) Li X, Cun L, Lian C, Zhong L, Chen Y, Liao J, et al. Highly enantioselective Michael addition of malononitrile to alphabeta-unsaturated ketones. Org Biomol Chem 2008; 6: 349-53; (b) Su Z, Lee HW, Kim CK. Theoretical investigation on mechanism of asymmetric Michael addition of malononitrile to chalcones catalyzed by Cinchona alkaloid aluminium(III) complex. Org Biomol Chem 2011; 9: 6402-9; (c) Nikishkin NI, Huskens J, Verboom W. Study on the Pd/C-Catalyzed (Retro-)Michael addition reaction of activated methylene compounds to electron- poor styrenes. Eur J Org Chem 2010; 2010: 6820-3; (d) Karamthulla S, Pal S, Khan MN, Choudhury LH. Synthesis of novel spiro[indoline-3,7’-pyrrolo[12-c]imidazole]-6’-carbonitrile derivatives in water using a regioselective sequential three component reaction. RSC Adv 2013; 3: 15576-81.

[22] (a) Ghorai MK, Tiwari DP. Enantioselective synthesis of 4,5-dihydropyrroles via domino ring-opening cyclization (DROC) of *N*-activated aziridines with malononitrile. J Org Chem 2013; 78: 2617-25; (b) Ghorai MK, Talukdar R, Tiwari DP. An efficient synthetic route to carbocyclic enaminonitriles via Lewis acid catalysed domino-ring- opening-cyclisation (DROC) of donor-acceptor cyclopropanes with malononitrile. Chem Commun 2013; 49: 8205-7; (c) Yang X, Fox T, Berke H. Synthetic and mechanistic studies of metal-free transfer

hydrogenations applying polarized olefins as hydrogen acceptors and amine borane adducts as hydrogen donors. Org Biomol Chem 2012; 10: 852-60.

[23] (a) Goel A, Chaurasia S, Dixit M, Kumar V, Prakash S, Jena B, et al. Donor-acceptor 9-uncapped fluorenes and fluorenones as stable blue light emitters. Org Lett 2009; 11: 1289-92; (b) Pzharskii AF, Soldatenkov AT, Katritzky AR. Heterocycles in life and society. Wiley. Second Edition: 218-9.

[24] Zhang Q, Ning Z. J, Tian H. 'Click' synthesis of starburst triphenylamine as potential emitting material. Dyes Pigments 2009; 81: 80-4.

[25] Goel A, Kumar V, Nag P, Bajpai V, Kumar B, Singh C, et al. Thermally stable nonaggregating pyrenylarenes for blue organic light-emitting devices. J Org Chem 2011; 76: 7474-81.

[26] Rest C, Mayoral MJ, Fucke K, Schellheimer J, Stepanenko V, Fernández G. Self-assembly and (hydro)gelation triggered by cooperative π–π and unconventional C-H…X hydrogen bonding interactions. Angew Chem Int Edit 2014; 53: 700-5.

[27] Chen Y, Lam JWY, Chen S, Tang BZ. Synthesis properties and applications of poly(ethylene glycol)-decorated tetraphenylethenes. J Mater Chem C 2014; 2: 6192-8.

[28] Anger P, Bharadwaj P, Novotny L. Enhancement and quenching of single-molecule fluorescence. Phys Rev Lett 2006; 96: 11302-5.

[29] Rodriguez-Romero J, Aparicio-Ixta L, Rodriguez M, Ramos-Ortiz G, Maldonado JL, Jimenez-Sanchez A, et al. Synthesis chemical-optical characterization and solvent interaction effect of novel fluorene-chromophores with D-A-D structure. Dyes Pigments 2013; 98: 31-41.

[30] Huang J, Zhao Y, Ding X, Jia H, Jiang B, Zhang Z, et al. Synthesis and charge-transporting properties of electron-deficient CN_2-fluorene based D-A copolymers. Polym Chem 2012; 3: 2170-7.

[31] (a) Jarowski PD, Wu YL, Boudon C, Gisselbrecht JP, Gross M, Schweizer WB, et al. New donor-acceptor chromophores by formal [2+2] cycloaddition of donor-substituted alkynes to dicyanovinyl derivatives. Org Biomol Chem 2009; 7: 1312-22; (b) Ramulu BJ, Chanda T, Chowdhury S, Nandi GC, Singh MS. Organocatalyzed straightforward synthesis of highly fluorescent 3,5-disubstituted 2,6-dicyanoanilines via domino annulation of α-enolicdithioesters with malononitrile. RSC Adv 2013; 3: 5345-9.

[32] (a) Peng L, Zhou ZJ, Wei RR, Li K, Song PS, Tong AJ. A fluorescent probe for thiols based on aggregation-induced emission and its application in live-cell imaging. Dyes Pigments 2014; 108: 24-31; (b) Hong YN, Lam JWY, Tang BZ. Aggregation-induced emission: phenomenon mechanism and applications. Chem Commun 2009; 29: 4332-53.

[33] (a) Wang J, Xu X, Shi L, Li L. Fluorescent organic nanoparticles based on branched small molecule: preparation and ion detection in lithium-ion battery. ACS Appl Mater Interfaces 2013; 5: 3392-400; (b) Pathak RK, Dessingou J, Hinge VK, Thawari AG, Basu SK, Rao CP. Quinoline driven fluorescence turn on 1,3-bis-calix[4]arene conjugate-based receptor to discriminate Fe^{3+} from Fe^{2+}. Anal Chem 2013; 85: 3707-14; (c) Yang B, Zhang XB, Liu WN, Hu R, Tan WH, Shen GL, et al. Fluorosurfactant-capped gold nanoparticles-based label-free colorimetric assay for Au^{3+} with tunable dynamic range via a redox strategy. Biosens Bioelectron 2013; 48: 1-5

[34] Wei TB, Zhang P, Shi BB, Chen P, Lin Q, Liu J, et al. A highly selective chemosensor for colorimetric detection of Fe^{3+} and fluorescence turn-on response of Zn^{2+}. Dyes Pigments 2013; 97: 297-302.

Table 1

Optimization of reaction conditions [a]

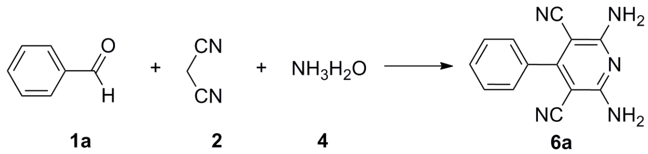

Entry	Solvent	Catalyst (equiv)	Time (h)	Temp (°C)	Yield (%) [b]
1	MeOH	NH_3 (1.0)	3	25	79
2	MeOH	NaOH (1.0)	20	25	35
3	MeOH	NaOMe (1.0)	20	25	27
4	MeOH	DBU (1.0)	48	25	Trace
5	MeOH	CH_3NH_2 (1.0)	20	25	5
6	MeOH	$(C_2H_5)_3N$ (1.0)	20	25	15
7	CH_2Cl_2	NH_3 (1.0)	10	25	20
8	CH_3CN	NH_3 (1.0)	10	25	23
9	THF	NH_3 (1.0)	10	25	35
10	EtOH	NH_3 (1.0)	3	25	72
11	H_2O	NH_3 (1.0)	3	25	46
12	Mixture[c]	NH_3 (1.0)	3	25	83
13	Mixture[c]	NH_3 (1.0)	3	40	85
14	Mixture[c]	NH_3 (1.0)	2	60	69
15	Mixture[c]	NH_3 (1.0)	2	80	42
16	Mixture[c]	NH_3 (1.0)	2	100	31

[a] Reaction conditions: benzaldehyde (10 mmol), malonoitrile (20 mmol), ammonia solution (20 mmol, 26~28 wt%). [b] Isolated yields. [c] $V_{MeOH}:V_{H2O} = 6:1$

Table 2

Three-componet one-pot synthesis of (Multi) donor-acceptor pyridnes derivatives **6**[a]

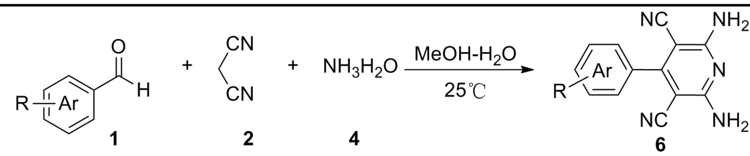

Entry	Ar	Time (h)	Product	Yield (%) [b]
1	Ph	3	**6a**	83
2	Pyridine-3-yl	3	**6b**	79
3	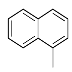	3.5	**6c**	84
4	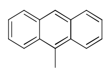	8	**6d**	85
5	4-Cl-Ph	4	**6e**	82
6	4-F-Ph	6	**6f**	80
7	4-Me-Ph	4.5	**6g**	82
8	4-OH-Ph	4	**6h**	79
9	3-NO_2-Ph	3	**6i**	76
10	2-Cl-Ph	5	**6j**	81
11	2-Et-Ph	5	**6k**	81
12	2-OH-Ph	6	**6l**	75
13	2-CN-Ph	5	**6m**	76
14	2,4-diCl-Ph	5	**6n**	77
15	2-F-6-Cl-Ph	2.5	**6o**	78

[a] Reaction conditions: aldehyde compounds (10 mmol), malonoitrile (20 mmol), ammonia solution (20 mmol, 26~28 wt%), MeOH (60 ml), H_2O (10 ml). [b] Isolated yields

Table 3

Photophysical properties of synthesized pyridine derivatives in different solvent

Compd	λ_{max}, abs[a] (nm)			λ_{max}, em[b] (nm)			PL
	H_2O [d]	DMSO [d]	THF [d]	H_2O [d]	DMSO [d]	THF [d]	Color[c]
6a	336 (0.20)	341 (0.24)	335 (0.37)	466 (141)	NF	NF	B
6c	333 (0.10)	337 (0.16)	332 (0.17)	376 (118)	415 (146)	400 (86)	B
6d	386 (0.13)	391 (0.08)	388 (0.10)	NF	417 (115)	NF	B
6e	335 (0.19)	339 (0.13)	333 (0.12)	NF	417 (107)	NF	B
6f	334 (0.22)	338 (0.15)	334 (0.12)	NF	NF	NF	NF
6g	333 (0.15)	339 (0.18)	334 (0.18)	NF	436(108)	NF	B
6h	334 (0.38)	338 (0.23)	334 (0.14)	NF	442(80)	NF	B
6i	336 (0.09)	339 (0.07)	336 (0.17)	NF	NF	NF	NF
6j	335 (0.27)	338 (0.33)	336 (0.35)	NF	NF	NF	NF
6k	333 (0.26)	337 (0.26)	332 (0.26)	NF	NF	NF	NF
6l	371 (0.17)	374 (0.17)	368 (0.18)	477 (67)	487 (99)	490 (84)	G
6m	481 (0.26)	493 (0.40)	489 (0.24)	NF	570 (92)	570 (92)	ORG
6n	326 (0.08)	332 (0.18)	329 (0.24)	NF	390 (96)	NF	B
6o	338 (0.37)	343 (0.26)	338 (0.24)	NF	NF	NF	NF

[a] Longest wavelength absorption maximum. [b] Fluorescence emission maximum. [e] Color of the emitted light: B (blue), G (green), ORG (orange), NF (no fluorescence). [d] concentration [6] = 20 uM

Table 4

Captions for the Figures and Schemes

Entry	Description of the illustration
Fig. 1.	Caystal structure of compound **6c** with THF solvent. Thermal ellipsoids are drawn at 30% level.
Fig. 2.	TG and DSC plots of **6a** and **6c** under N_2 atmosphere.
Fig. 3.	Packing diagram of compound **6c**.
Fig. 4.	Photographs of the fluorescence emission of **6a** in solvent and non-solvent solution taken under UV light (365 nm, insert figure) and their fluorescence spectrums emission (λex = 336 nm); [**6a**] = 30 uM.
Fig. 5.	(a) Photographs taken under 365 nm UV lamb and (b) emission spectra of **6a** in THF-water mixtures with different water fractions (*f*w), [**6a**] = 50 uM; (c) fluorescence spectrums emission against the **6a** concentration in the range of 2-100 uM in aqueous solution (λex = 336 nm).
Fig. 6.	UV-vis absorption spectra (a) and fluorescence emission excited at 336 nm (b) of compound **6a**, **6l**, **6m** in THF solution at room temperature with the same concentration of 30 uM.
Fig. 7.	Various metal ions (100 uM) response for **6a** (10 uM) in the absence and presence of 100 uM of Au^{3+} in aqueous solution (λex/em = 336/466 nm).
Fig. 8.	Fluorescence spectra of **6a** (10 uM) upon the addition of Au^{3+} (0.3-100 uM) in aqueous solution (λex = 336 nm) and fluorescence intensity at 466nm plots against [Au^{3+}] according to fluorescence titration spectra.
Scheme 1.	Methods for the synthesis of compound **6**.
Scheme 2.	The synthetic design of 4-aryl-2,6-diamino-3,5-dicyanopyridine.
Scheme 3.	The proposed mechanism for the formation of **6a**.

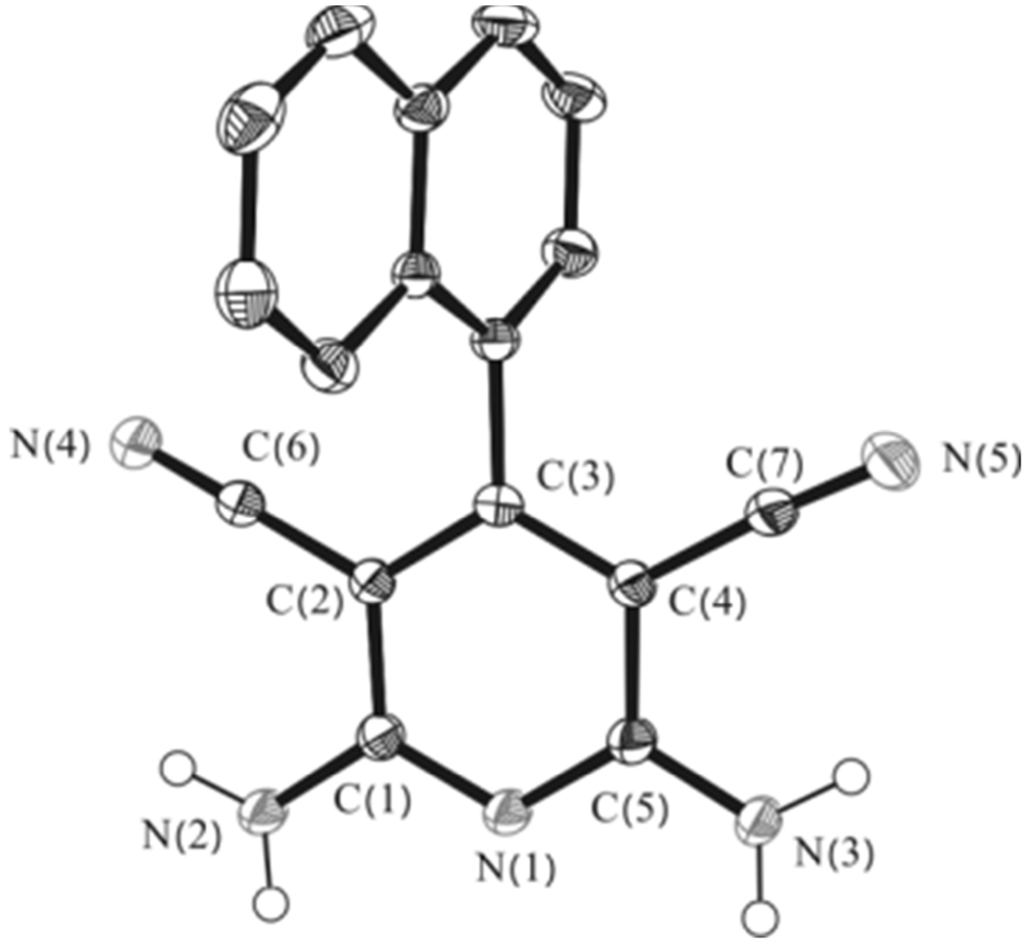
N(4)
C(6)
C(3)
C(7)
N(5)
C(2)
C(4)
C(1)
C(5)
N(2)
N(1)
N(3)

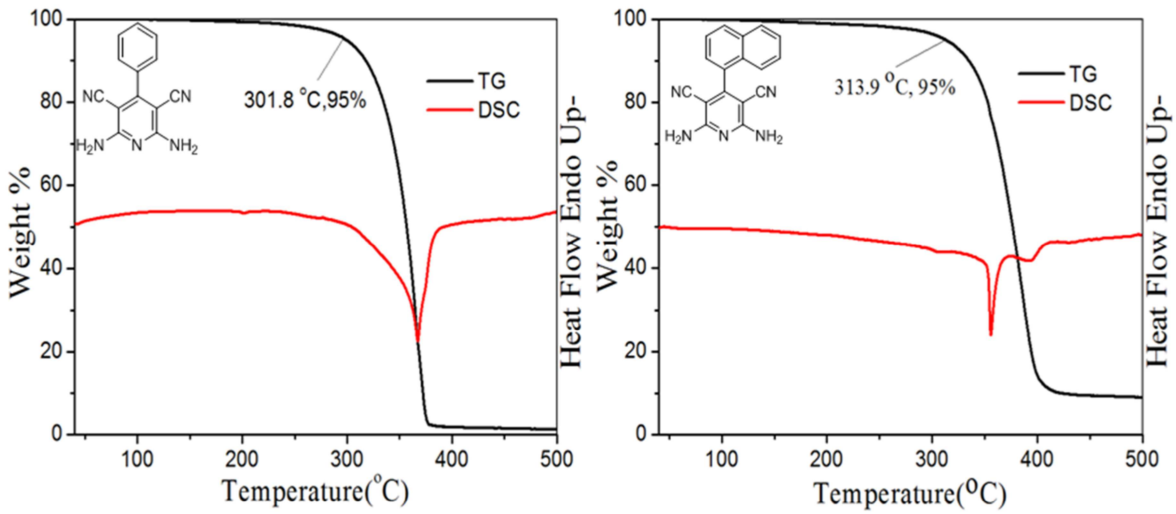

100
80
60
40
20
0
Weight %
NC
CN
H2N
N
NH2
301.8 °C,95%
TG
DSC
Heat Flow Endo Up-
100
200
300
400
500
Temperature(°C)
313.9 °C, 95%

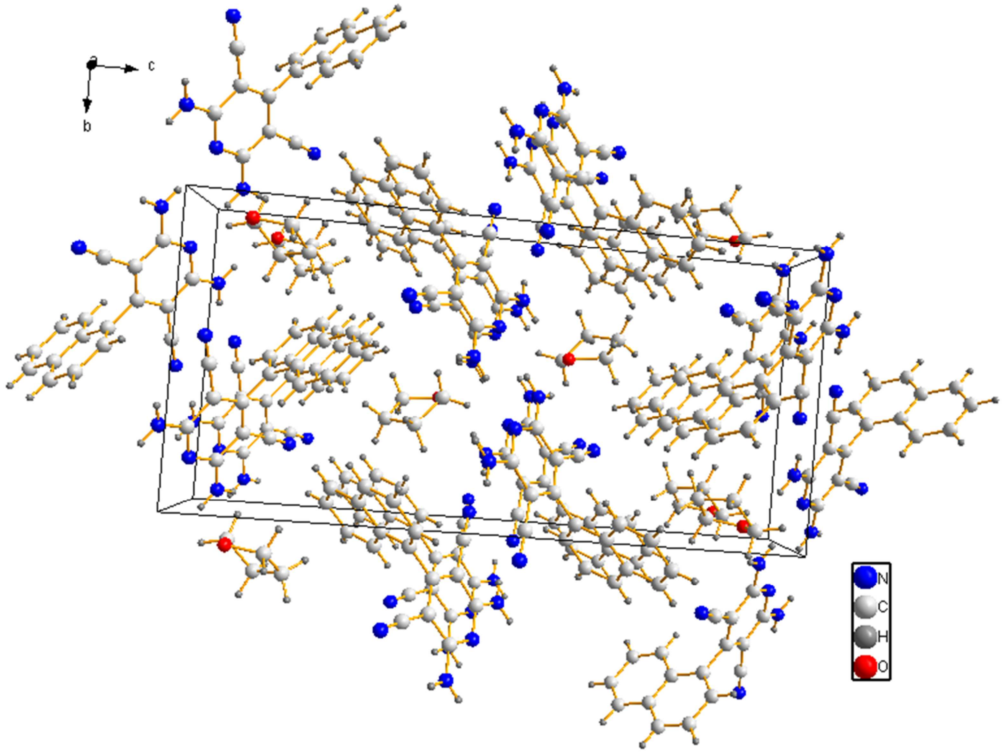

c
b
N
C
H
O

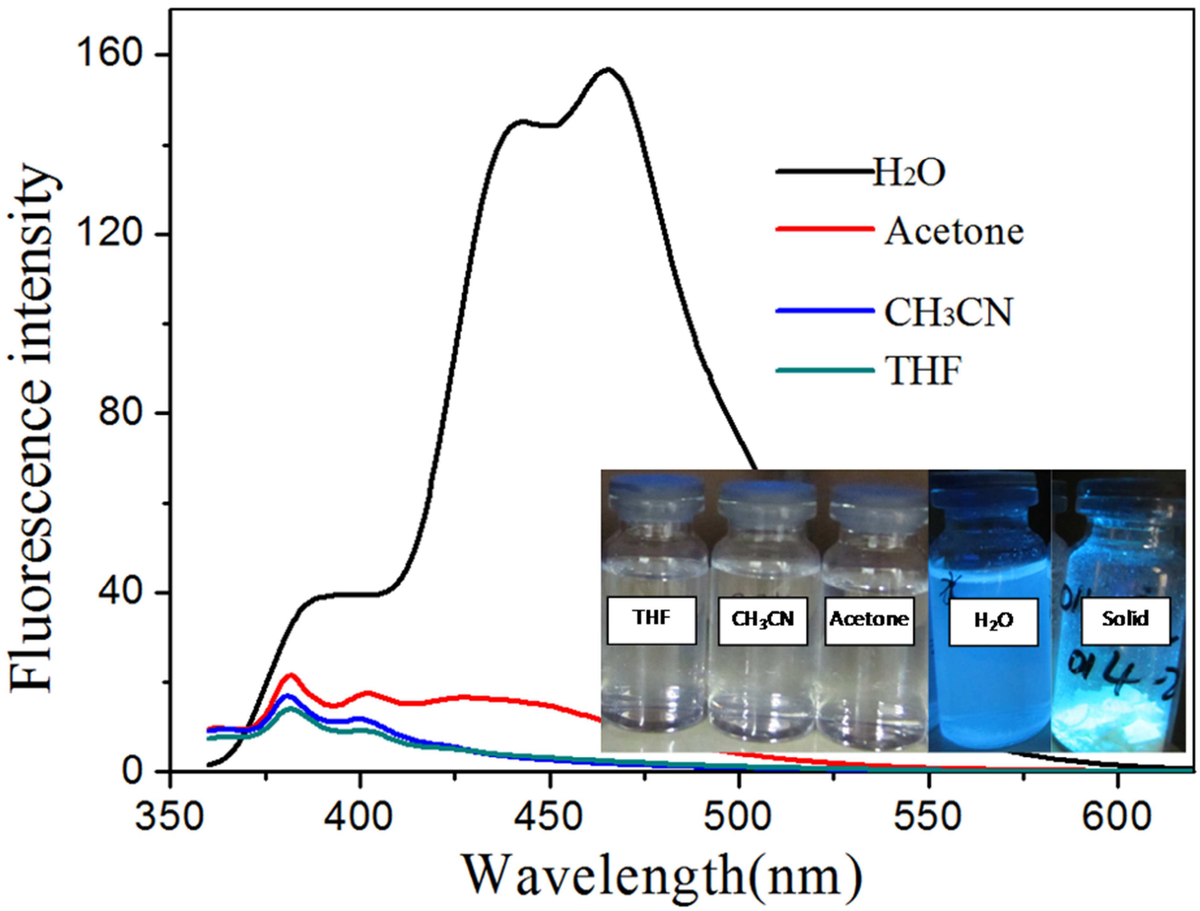

Fluorescence intensity
Wavelength(nm)
0
40
80
120
160
350
400
450
500
550
600
H2O
Acetone
CH3CN
THF
THF
CH3CN
Acetone
H2O
Solid

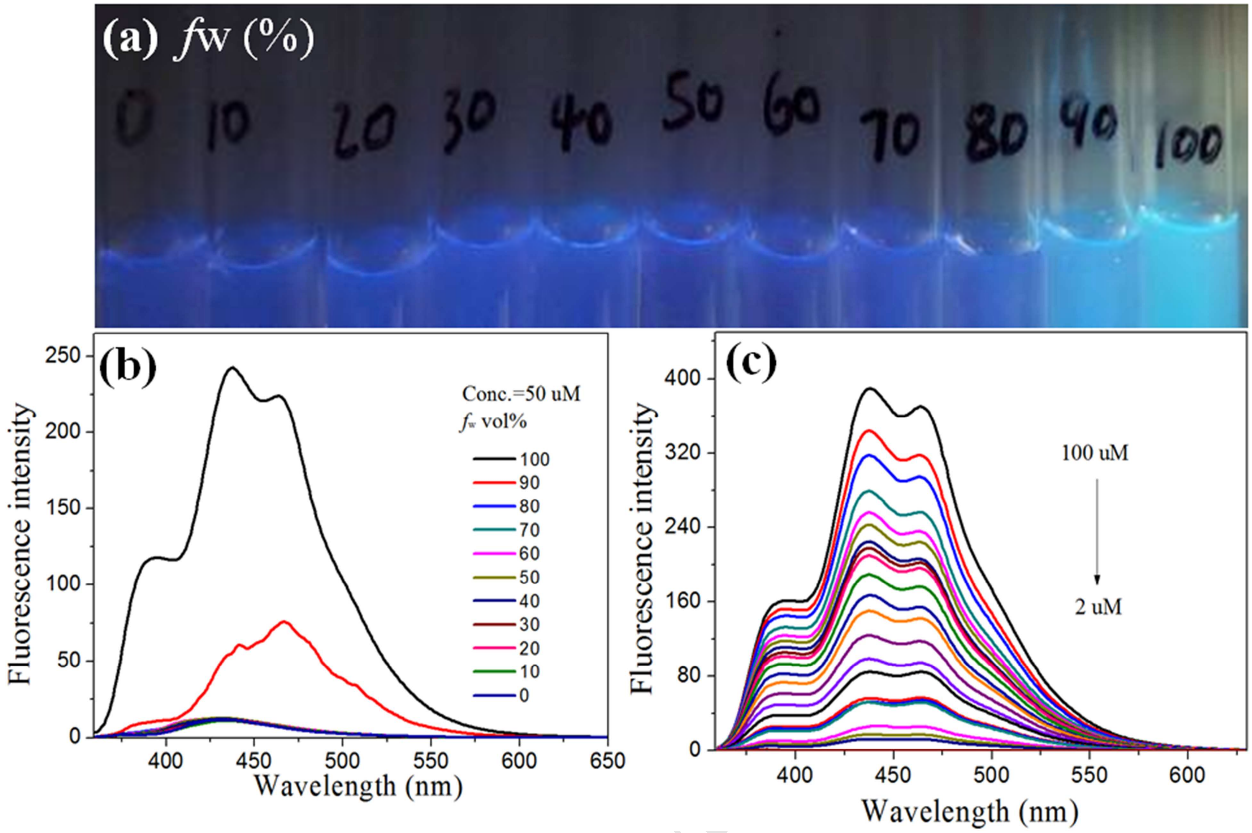
(a) fw (%)
0
10
20
30
40
50
60
70
80
90
100
(b)
Conc.=50 uM
fw vol%
100
90
80
70
60
50
40
30
20
10
0
Fluorescence intensity
Wavelength (nm)
(c)
100 uM
2 uM
Fluorescence intensity
Wavelength (nm)

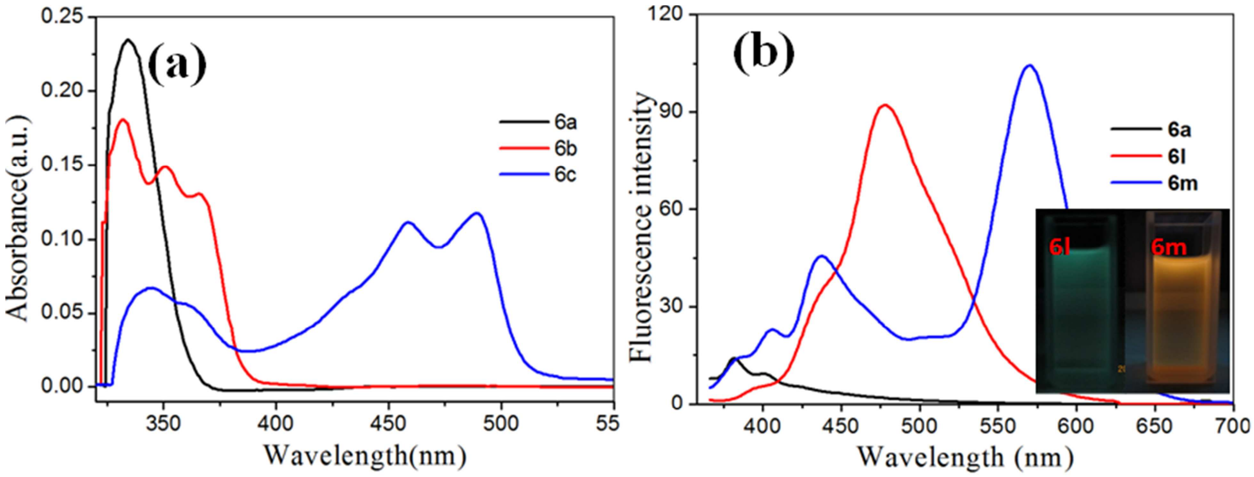
(a)
Absorbance(a.u.)
Wavelength(nm)
6a
6b
6c
0.25
0.20
0.15
0.10
0.05
0.00
350
400
450
500
55
(b)
Fluorescence intensity
Wavelength (nm)
6a
6l
6m
6l
6m
120
90
60
30
0
400
450
500
550
600
650
700

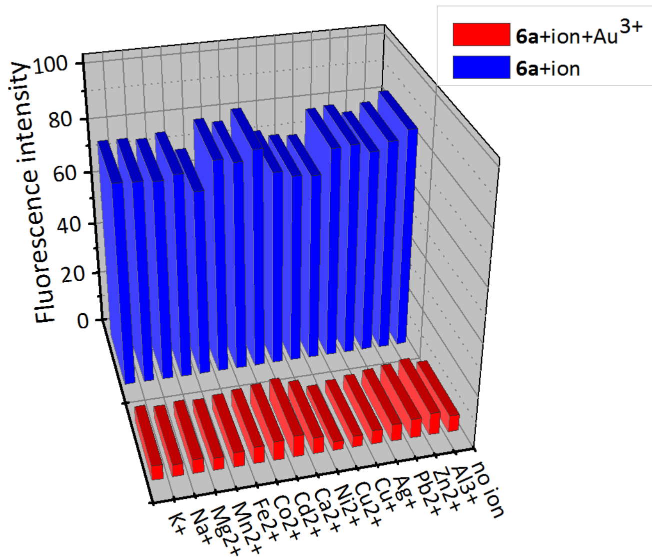
6a+ion+Au3+
6a+ion
Fluorescence intensity
100
80
60
40
20
0
K+
Na+
Mg2+
Mn2+
Fe2+
Co2+
Cd2+
Ca2+
Ni2+
Cu2+
Cu+
Ag+
Pb2+
Zn2+
Al3+
no ion

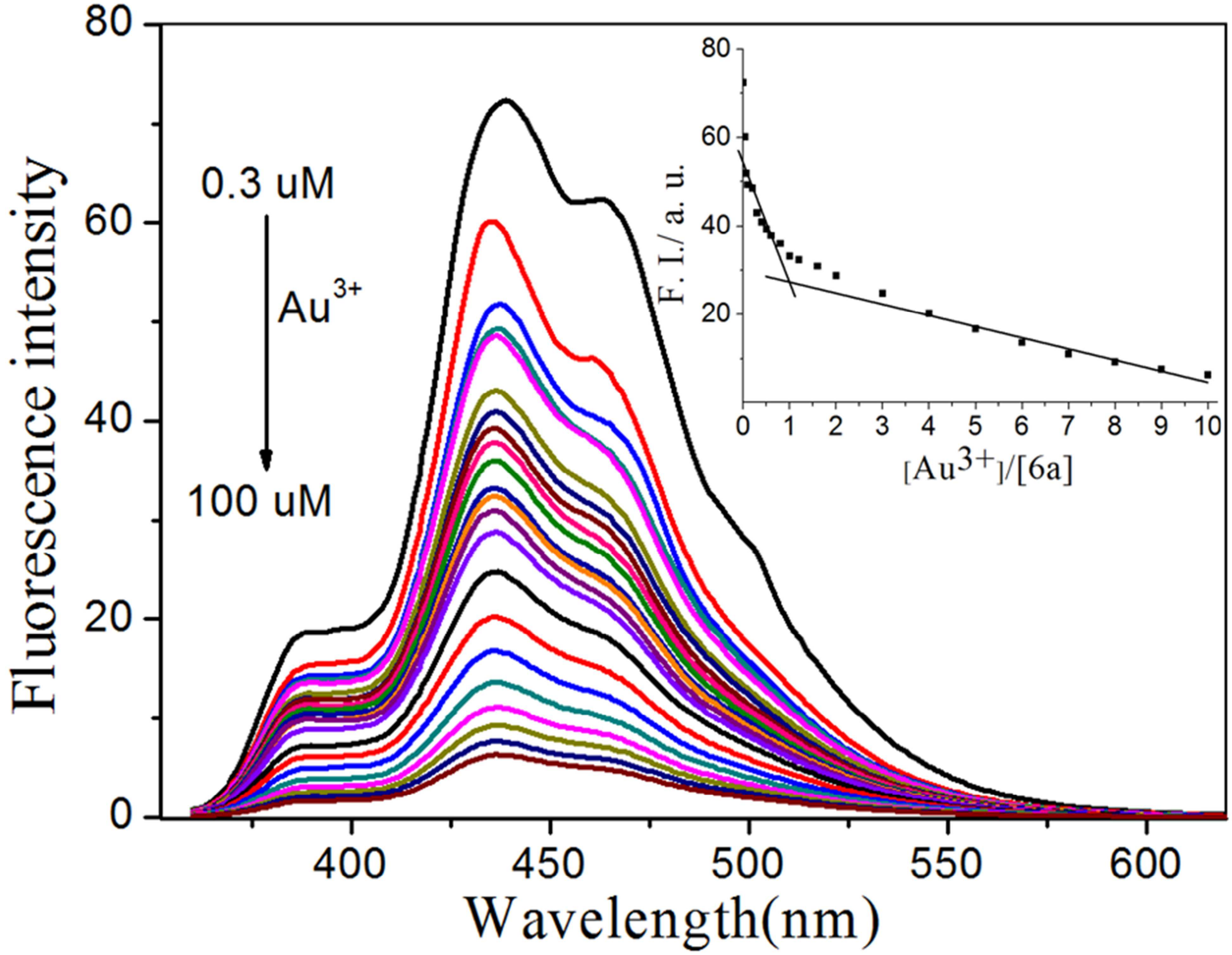

80
60
40
20
0
Fluorescence intensity
0.3 uM
Au3+
100 uM
400
450
500
550
600
Wavelength(nm)
F. I./ a. u.
[Au3+]/[6a]
0
1
2
3
4
5
6
7
8
9
10

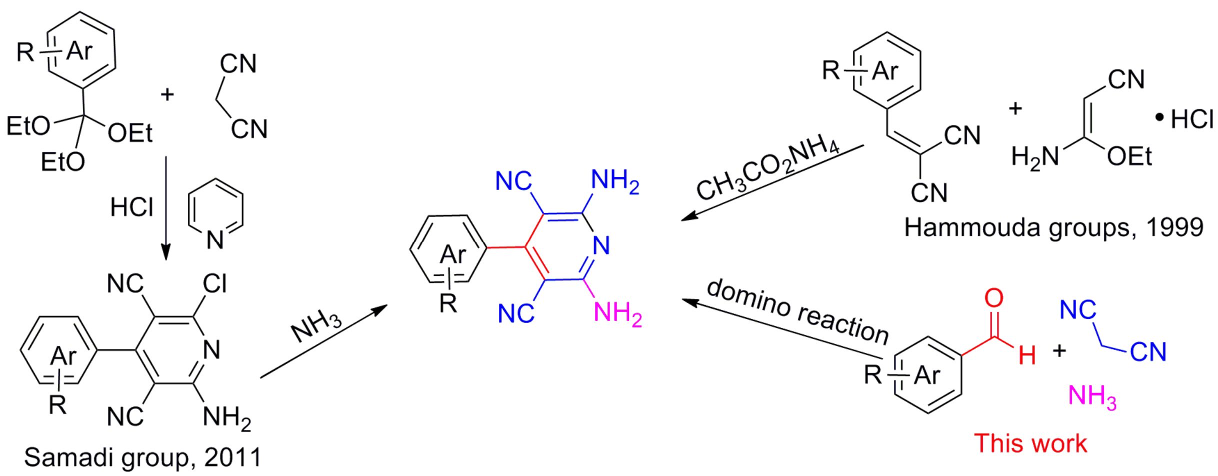

R
Ar
EtO
OEt
EtO
+
CN
CN
HCl
N
NC
Cl
N
NH2
NC
Samadi group, 2011
NH3
NC
NH2
N
NH2
NC
CH3CO2NH4
CN
CN
+
CN
H2N
OEt
• HCl
Hammouda groups, 1999
domino reaction
O
H
+
NC
CN
NH3
This work

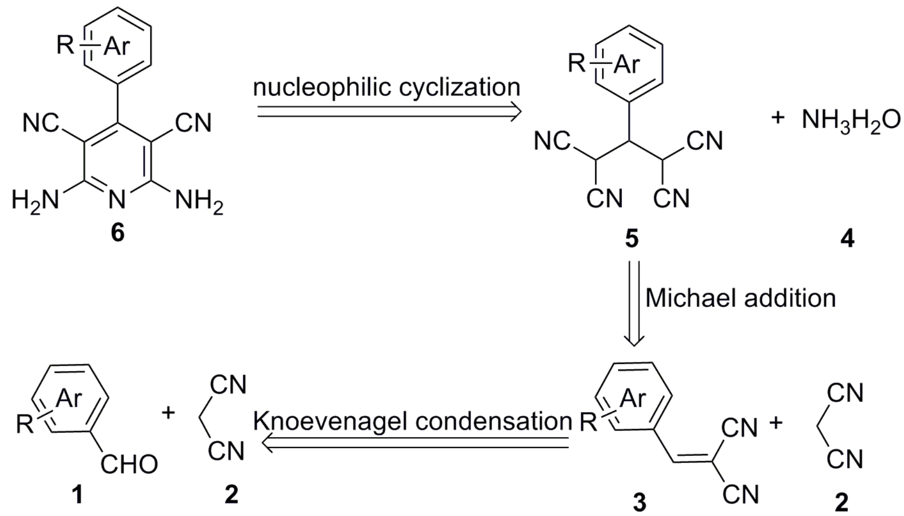

nucleophilic cyclization
Michael addition
Knoevenagel condensation
R
Ar
NC
CN
H2N
N
NH2
6
5
+ NH3H2O
4
CHO
1
2
3

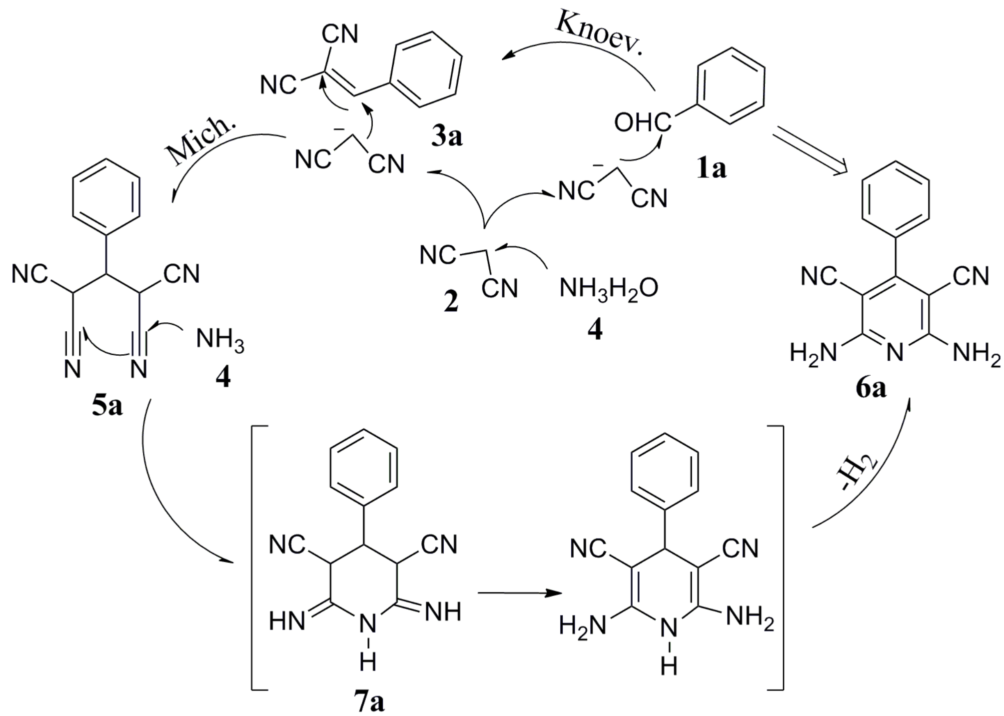
Knoev.
1a
3a
Mich.
2
4
NH$_3$H$_2$O
NH$_3$
5a
6a
7a
-H$_2$

Highlights

- A new series of pyridine derivative dyes were synthesized by domino reaction.
- The dyes exhibit the high aggregation-induced emission features.
- The dyes can be applied as fluorescent probe for detection the Au^{3+}.
- The probe can be applied in aqueous solution with high selectivity and sensitivity.

Supporting information

Synthesis, Optical Properties of Multi Donor-Acceptor Substituted AIE Pyridine Derivatives Dyes and Application for Au^{3+} Detection in Aqueous Solution

Junjuan Yang, Jiarong Li, Pengfei Hao, Fadong Qiu, Mingxing Liu, Qi Zhang, and Daxin Shi*

School of Chemical Engineering and Environment, Beijing Institute of Technology, Beijing, 100081, China
Fax: (+86)-010-68918012; E-mail: shidaxin@bit.edu.cn

Table of Contents

1. The ^1H NMR titration spectra of 6a in D_2O-[D_8]THF mixtures

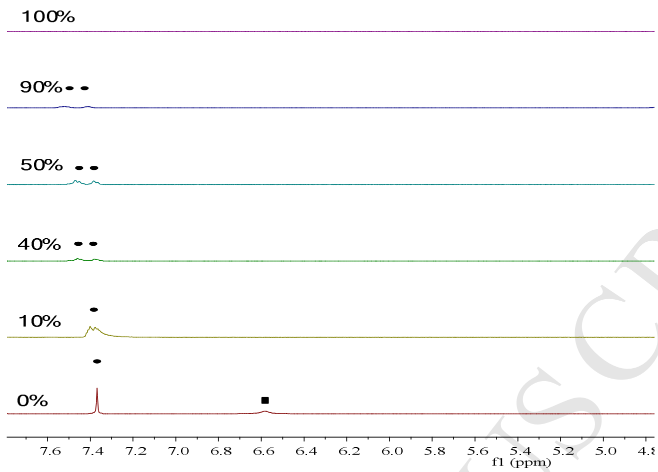

Fig. S1 The ^1H NMR titration spectra of **6a** in D_2O-[D_8]THF mixtures with different D_2O fractions (v/v, 0%, 10%, 40%, 50%, 90%, 100%). Proton signals correspond to the phenyl ring(•) and amino groups(▪).

2. ESI-MS spectra of the complex

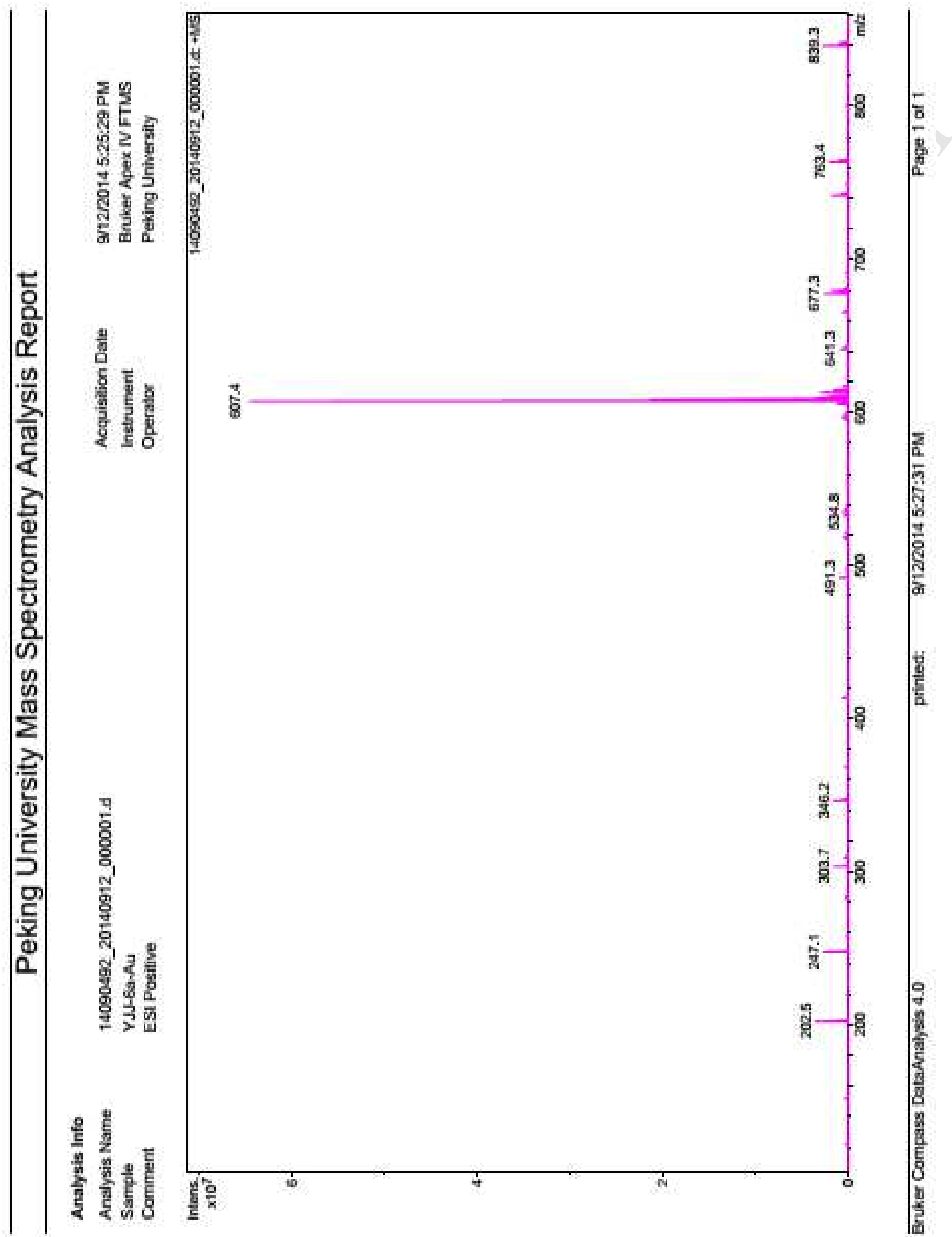

Fig. S2 ESI-MS spectra of the complex

3. The detection limit of 6a toward Au^{3+} ions

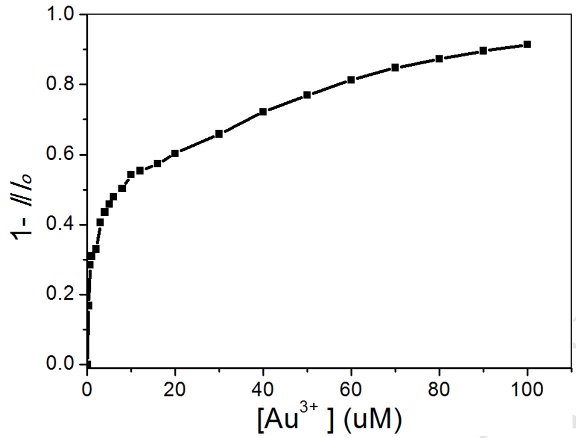

Fig. S3 The change of PL intensity of 6a aqueous solutio(10 uM) versus Au^{3+} concentration in a wide range of 0.3 uM to 100 uM.

4. Copies of ^{1}H NMR and ^{13}C NMR spectra

^{1}H NMR spectrum of **3a**

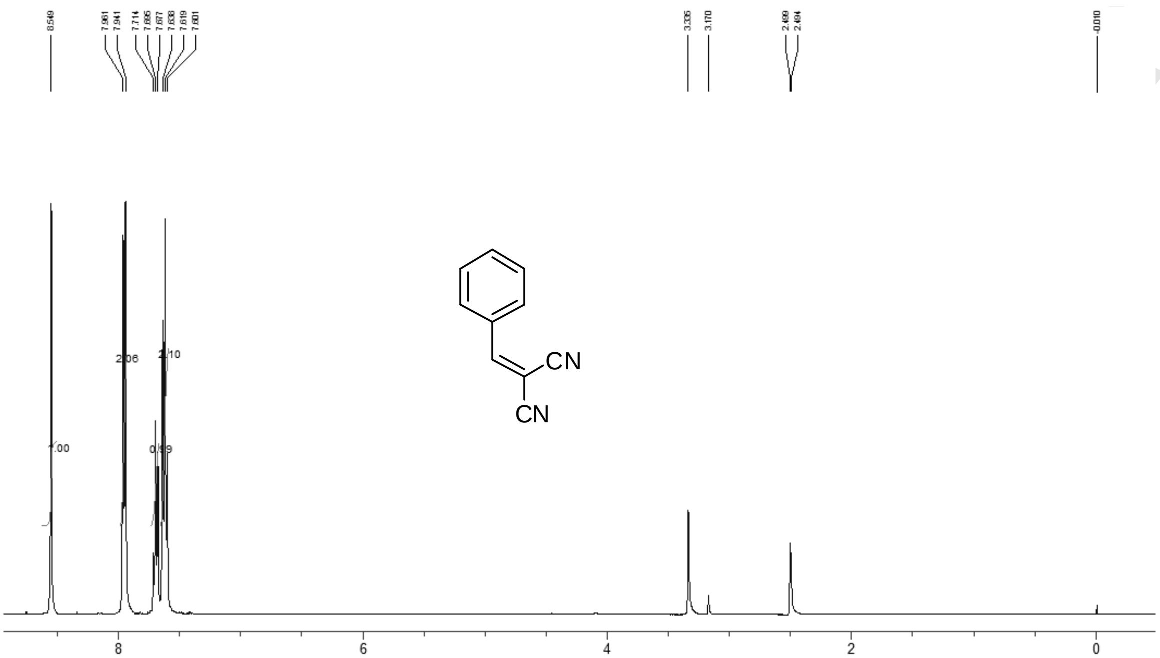

^{13}C NMR spectrum of **3a**

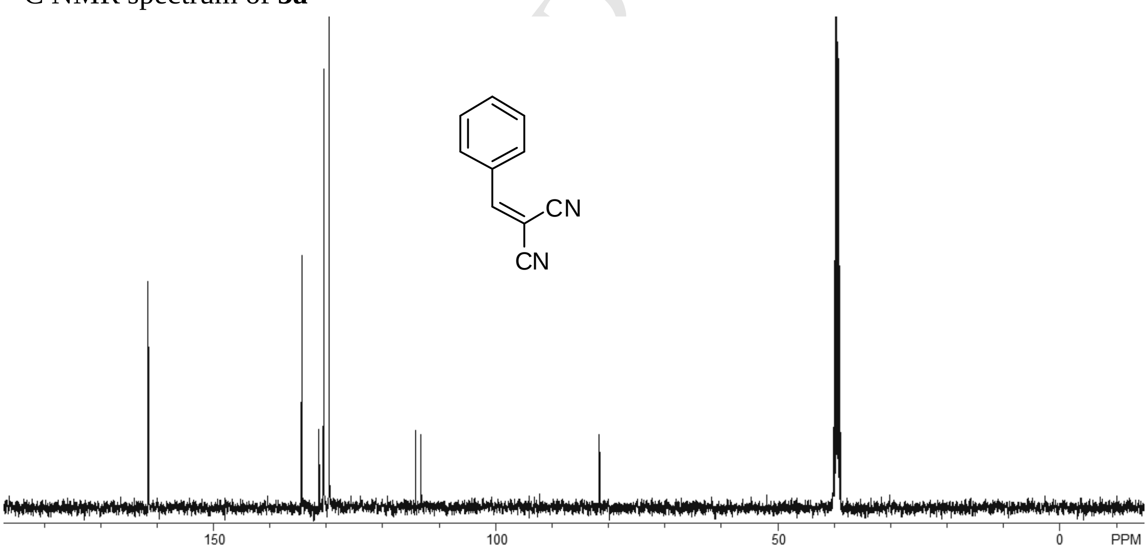

^{1}H NMR spectrum of **6a**

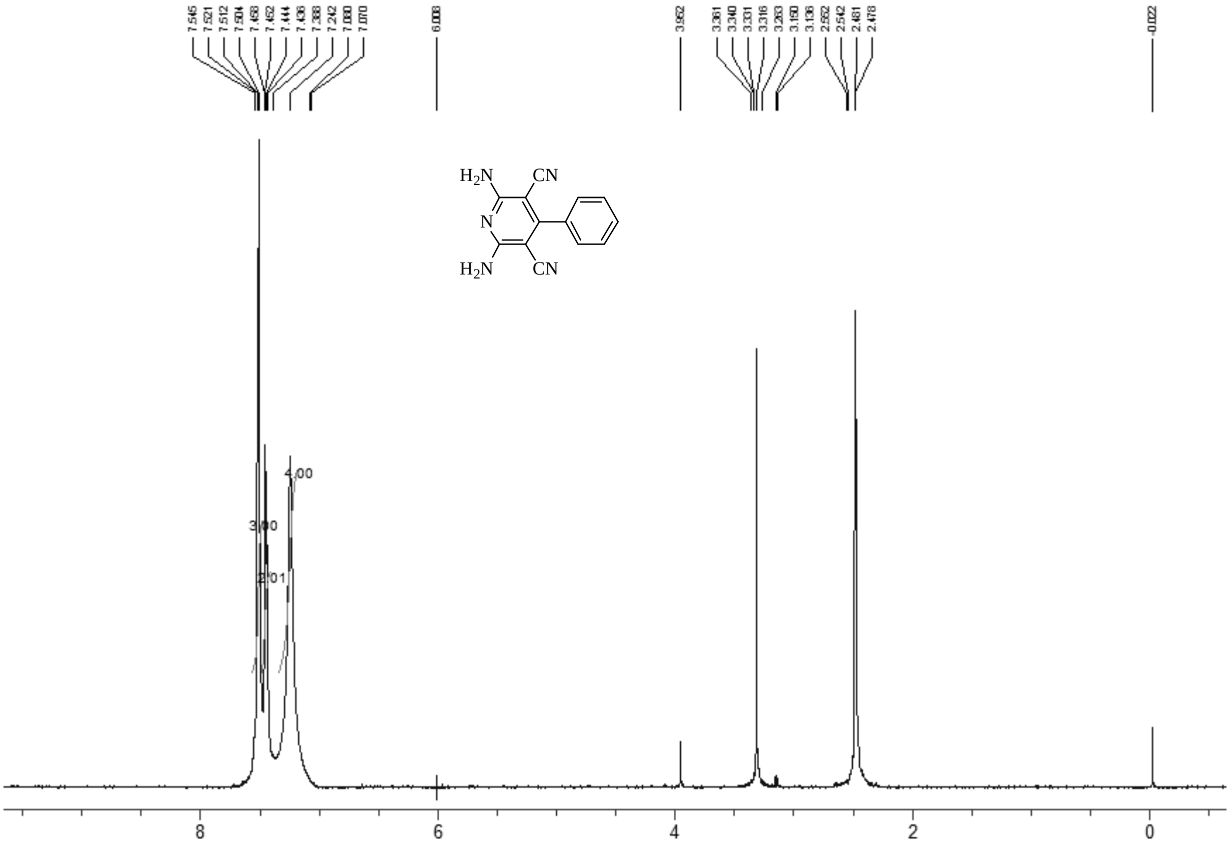

^{13}C NMR spectrum of **6a**

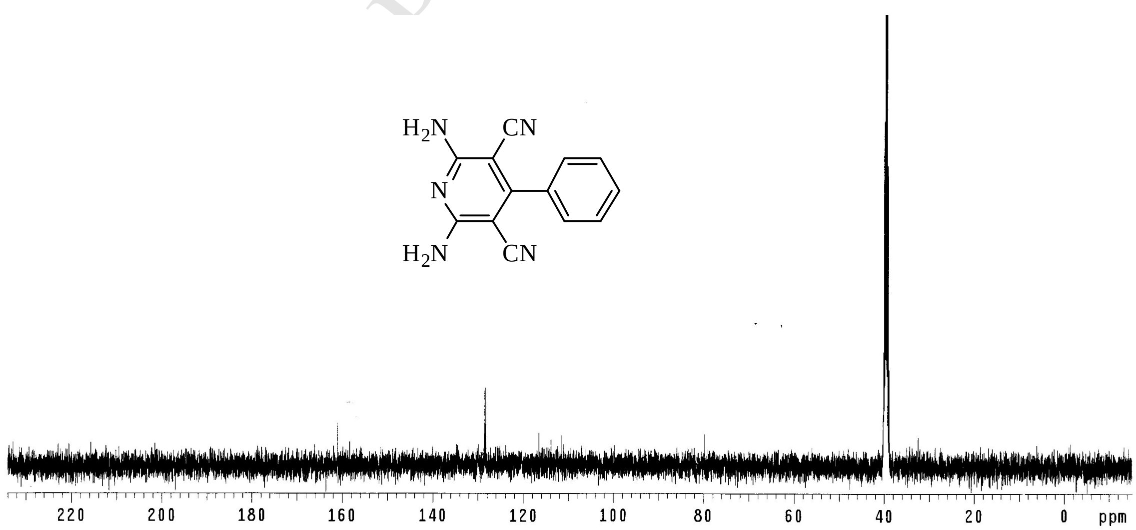

[1]H NMR spectrum of **6b**

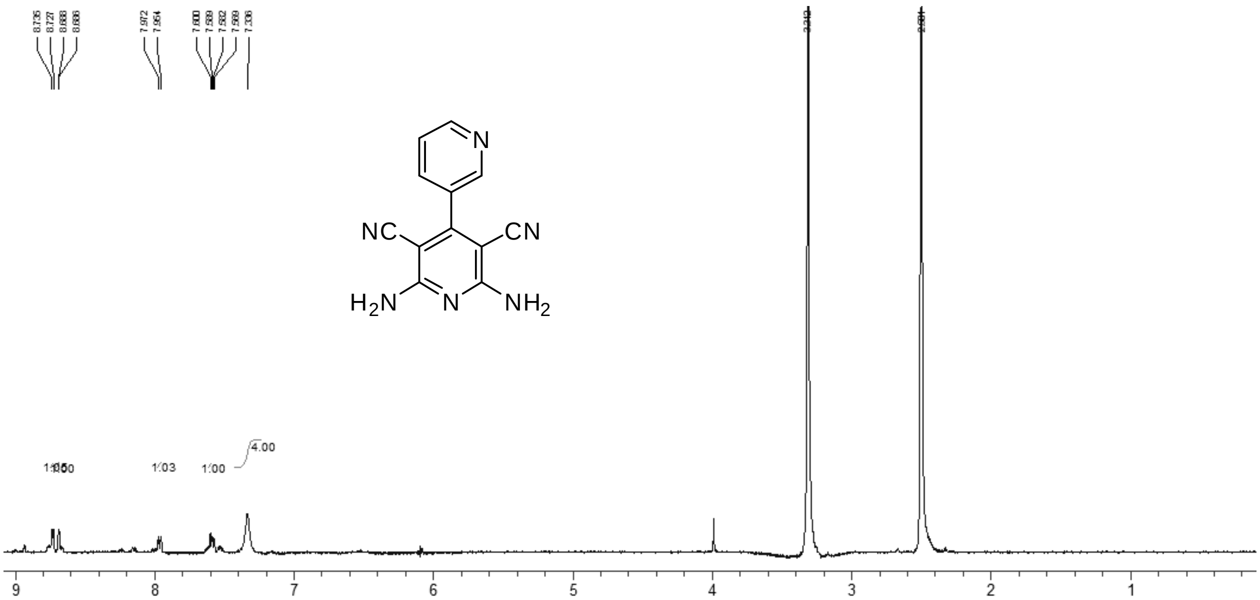

[13]C NMR spectrum of **6b**

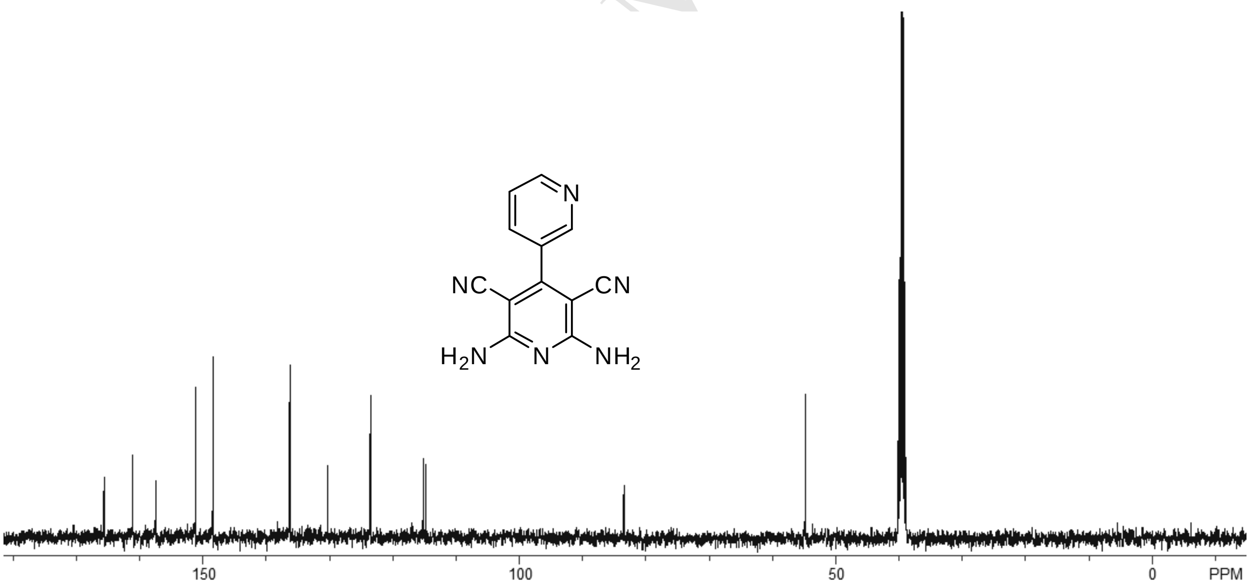

^{1}H NMR spectrum of **6c**

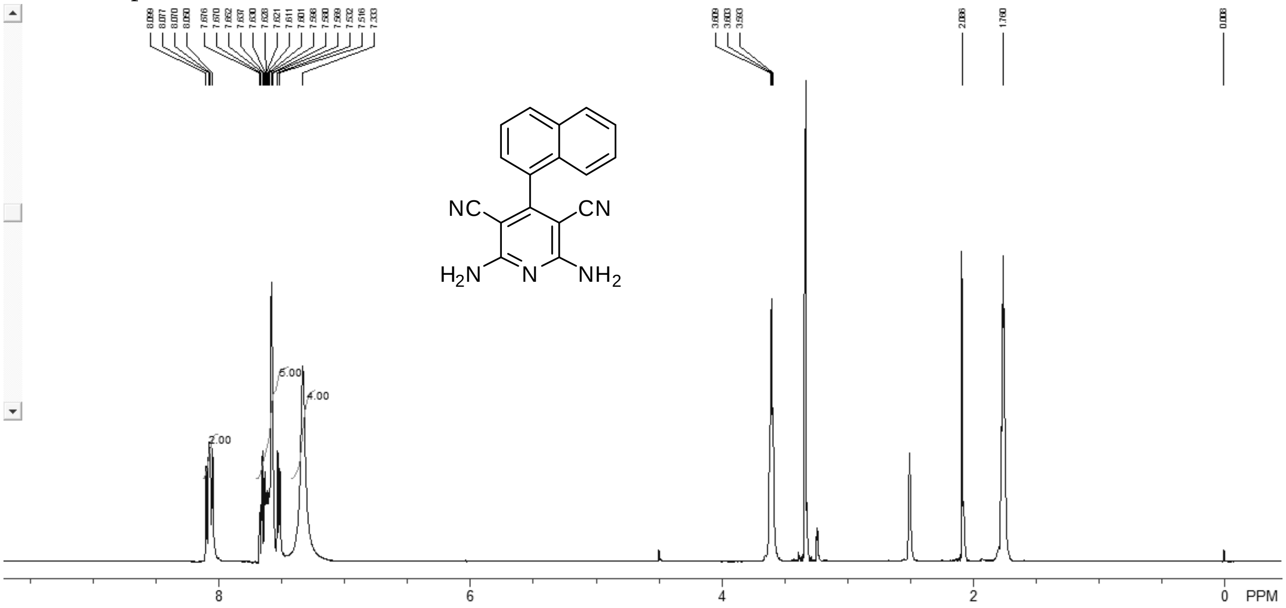

^{13}C NMR spectrum of **6c**

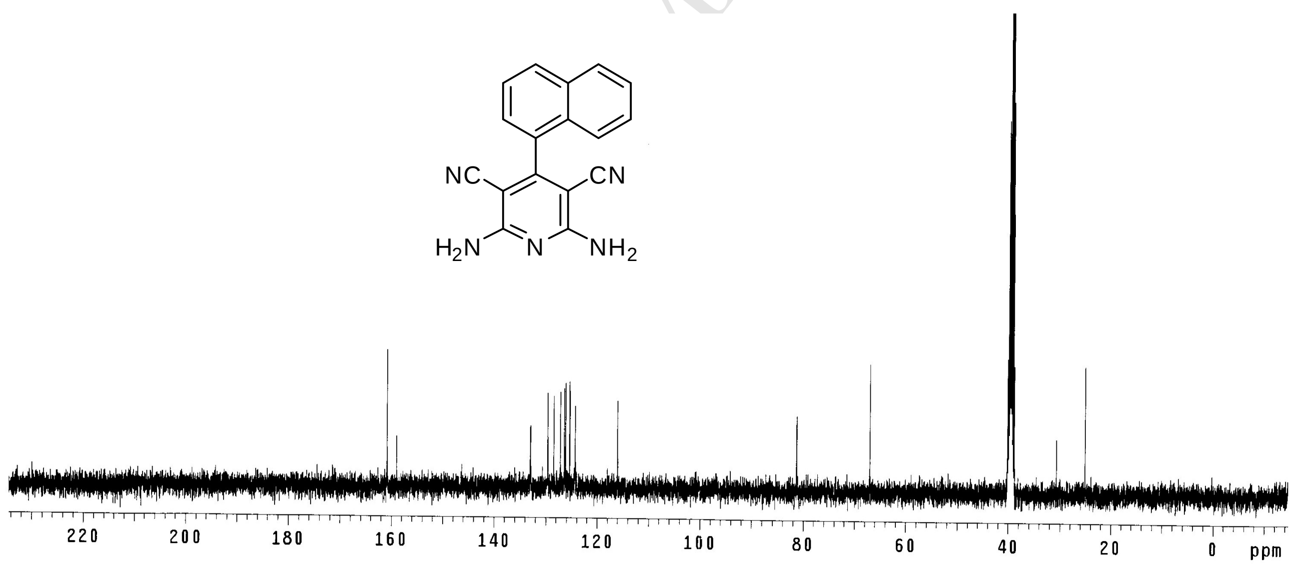

^{1}H NMR spectrum of **6d**

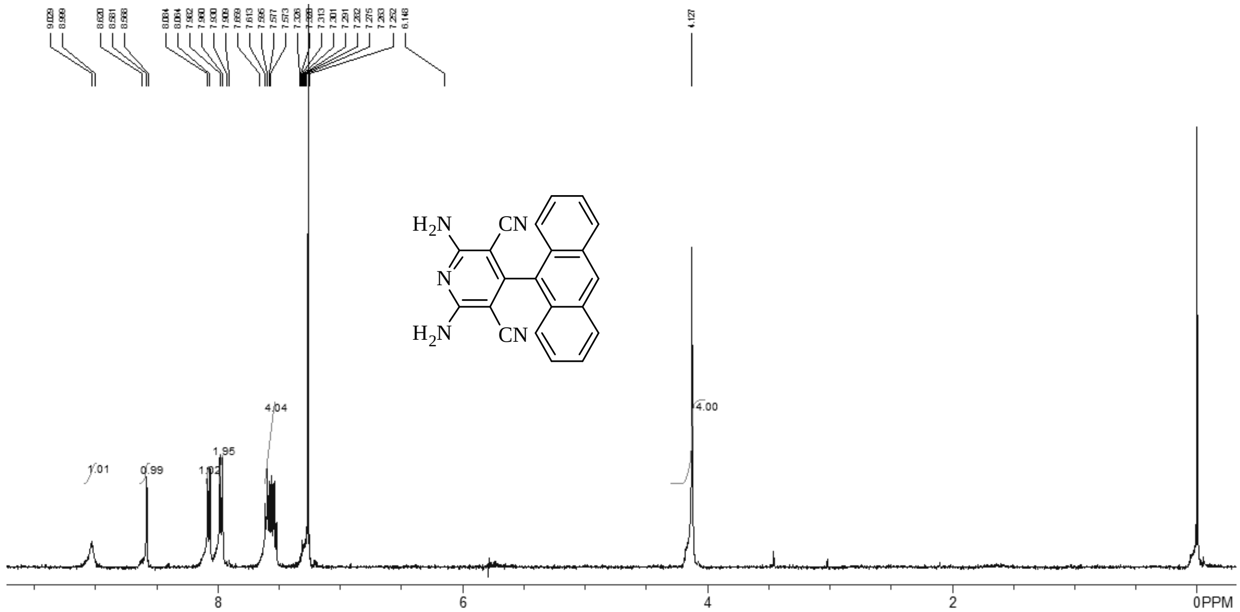

^{13}C NMR spectrum of **6d**

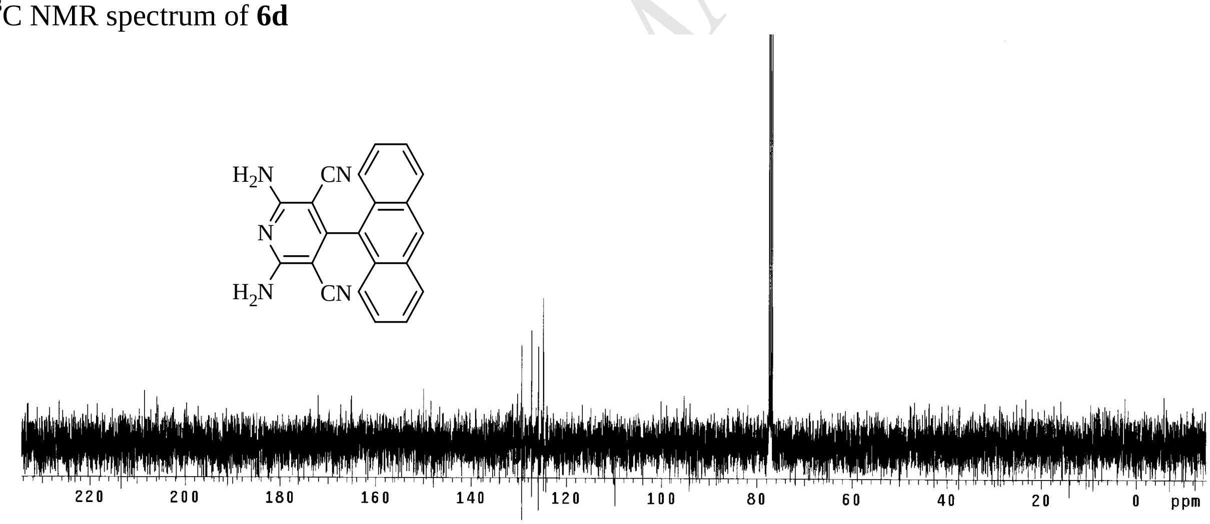

^{1}H NMR spectrum of **6e**

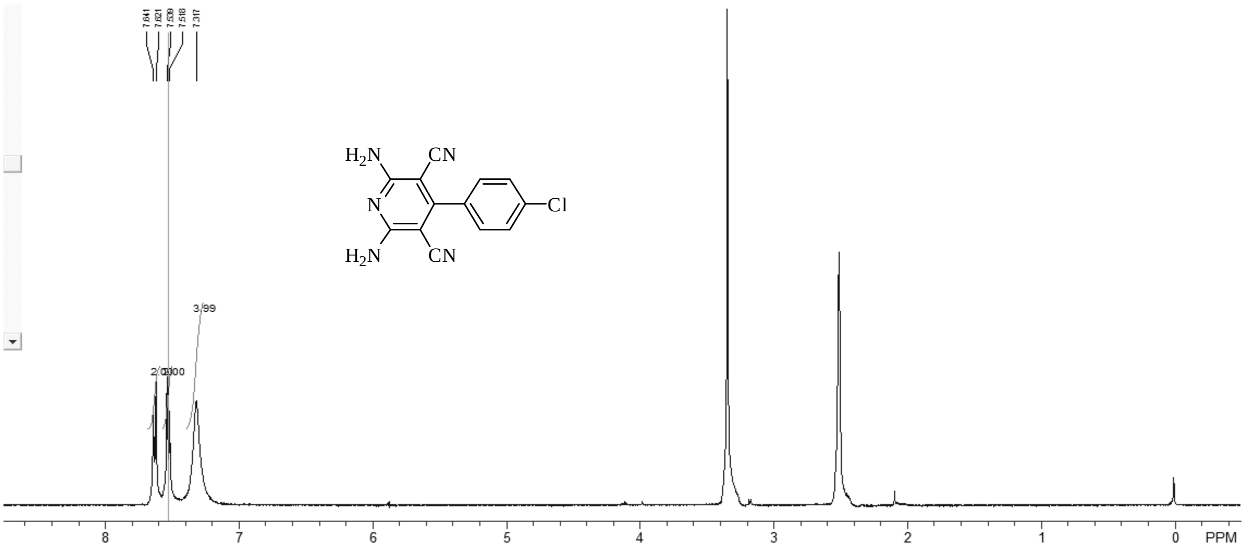

^{13}C NMR spectrum of **6e**

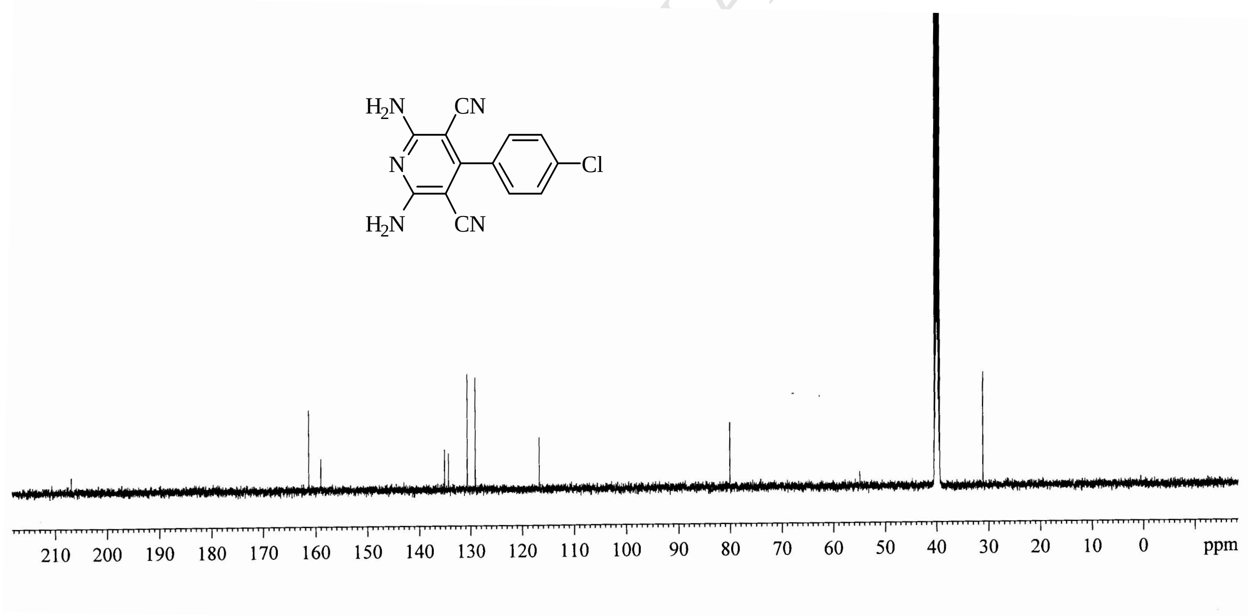

^{1}H NMR spectrum of **6f**

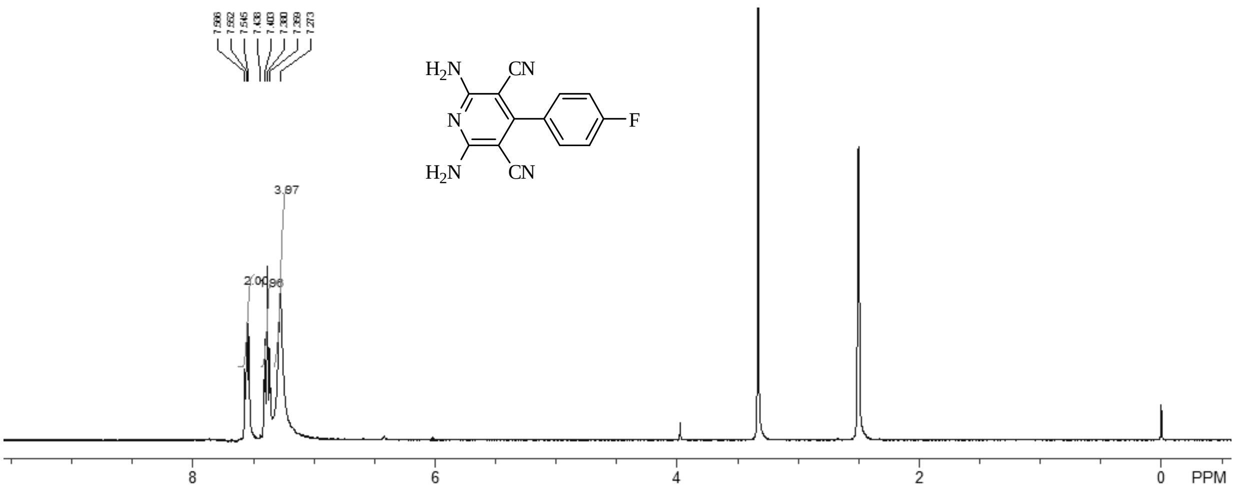

^{13}C NMR spectrum of **6f**

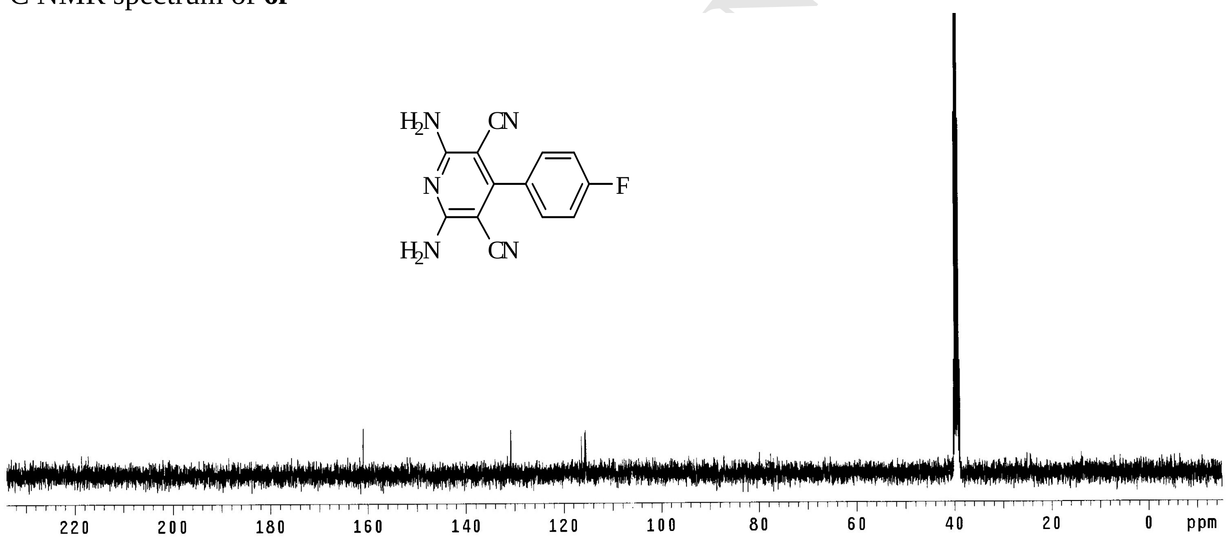

^{1}H NMR spectrum of **6g**

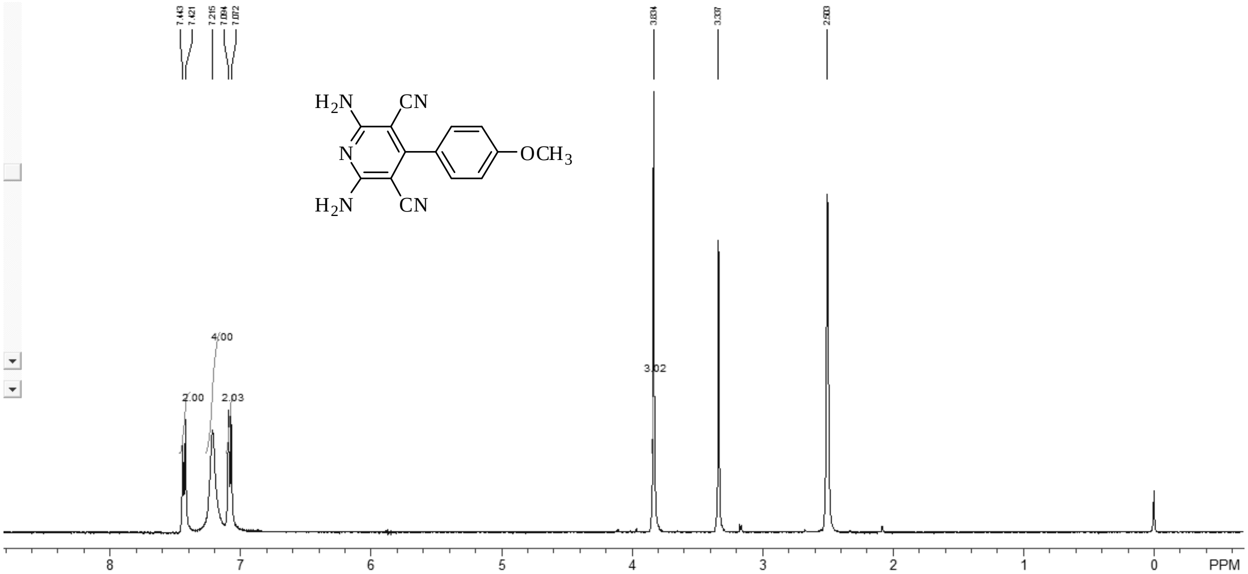

^{13}C NMR spectrum of **6g**

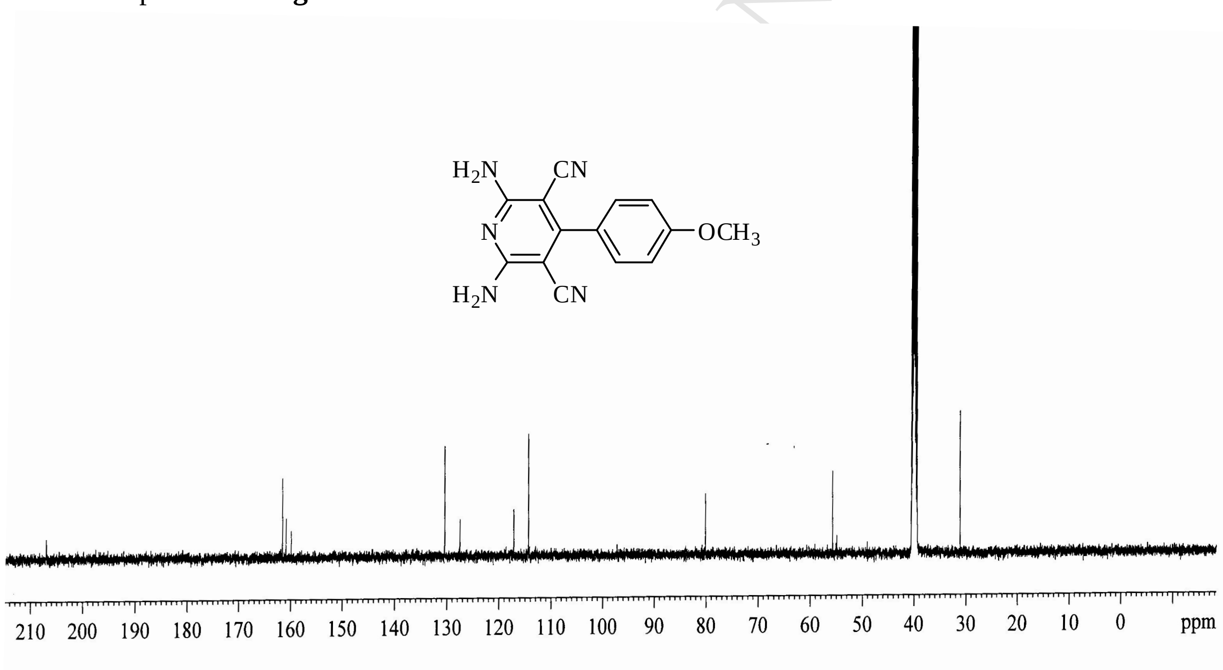

[1]H NMR spectrum of **6h**

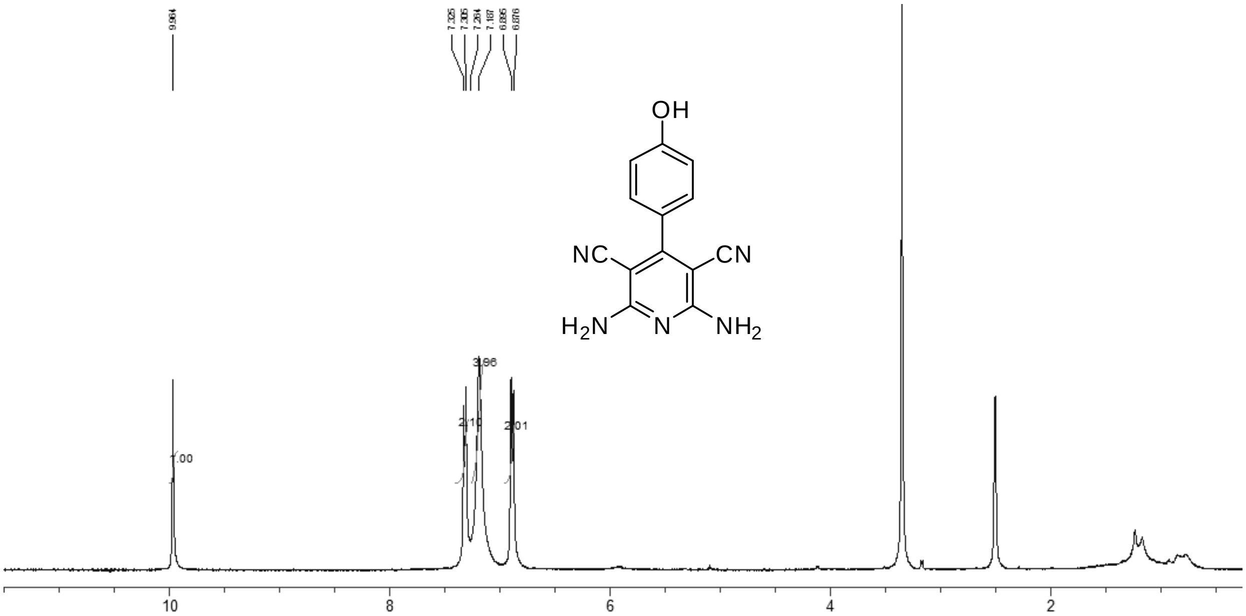

[13]C NMR spectrum of **6h**

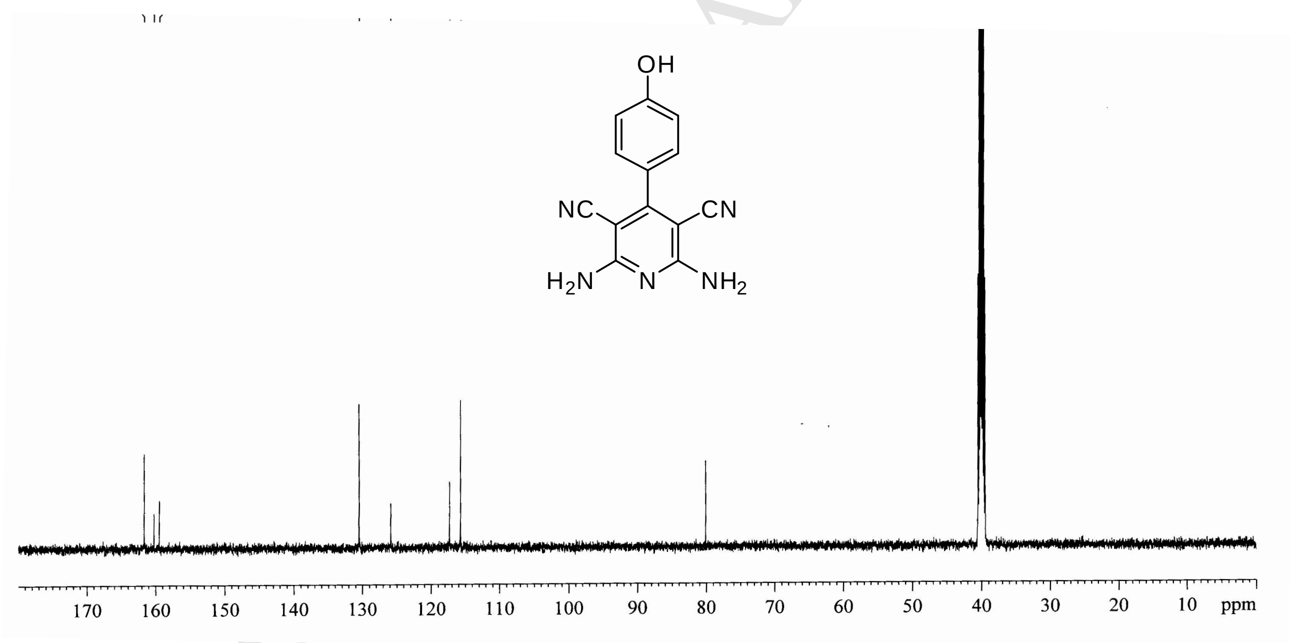

^{1}H NMR spectrum of **6i**

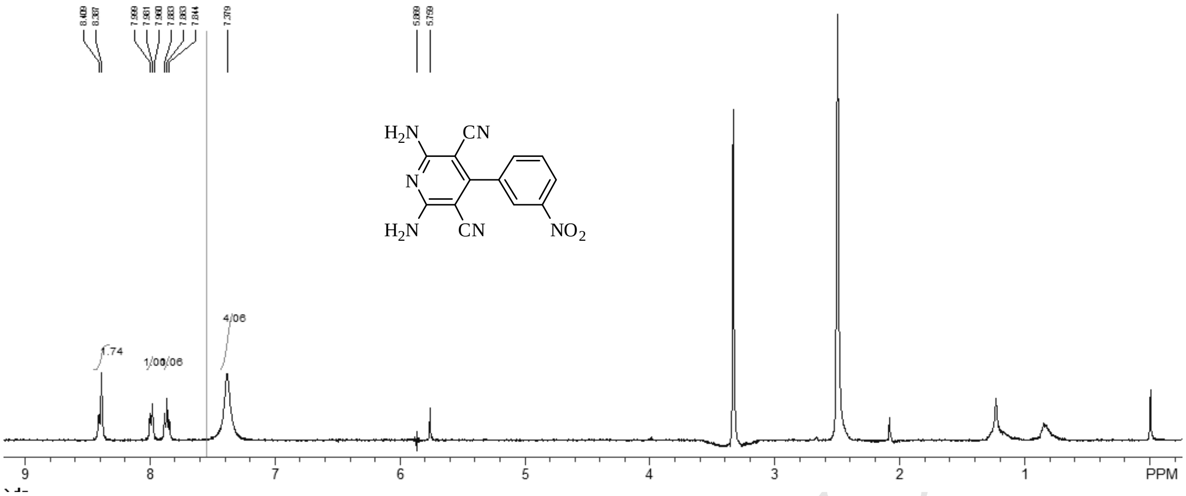

^{13}C NMR spectrum of **6i**

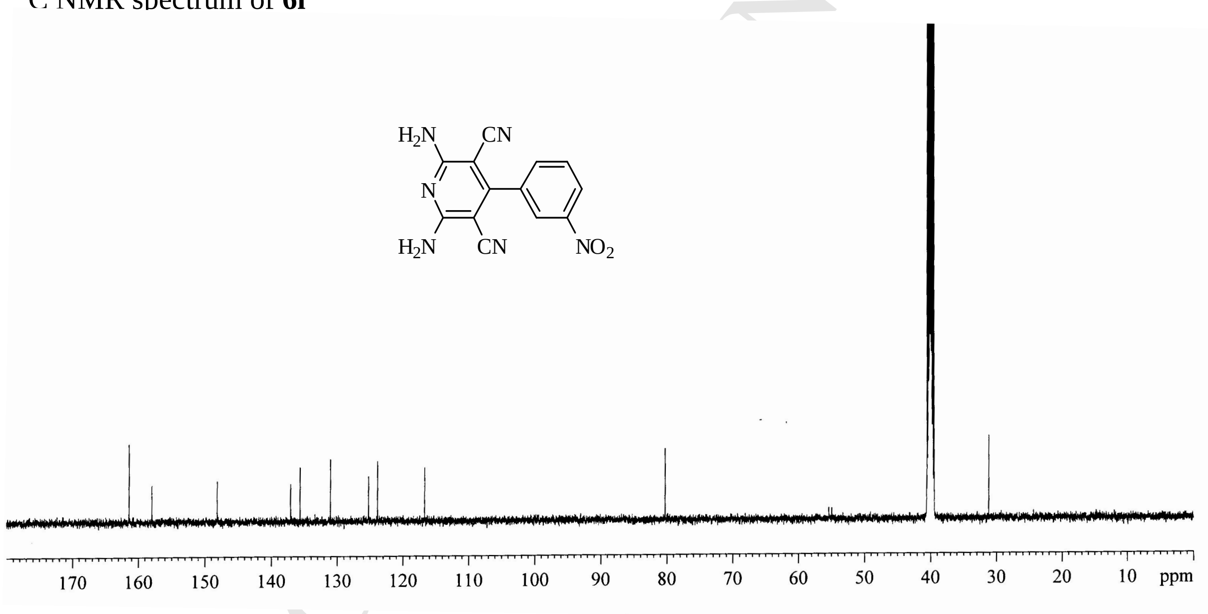

^{1}H NMR spectrum of **6j**

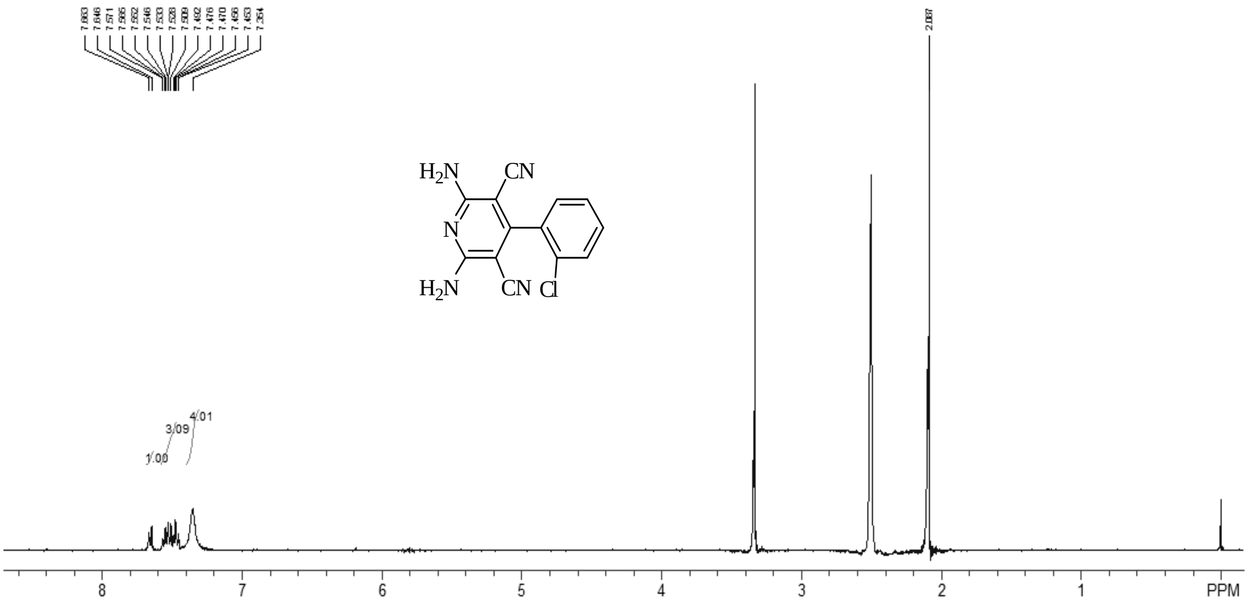

^{13}C NMR spectrum of **6j**

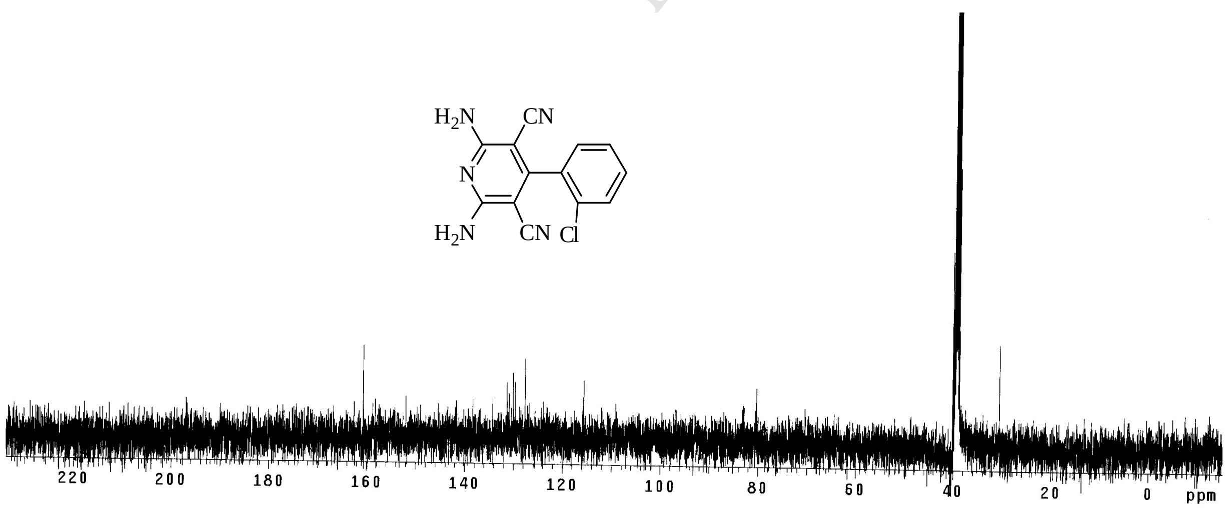

^{1}H NMR spectrum of **6k**

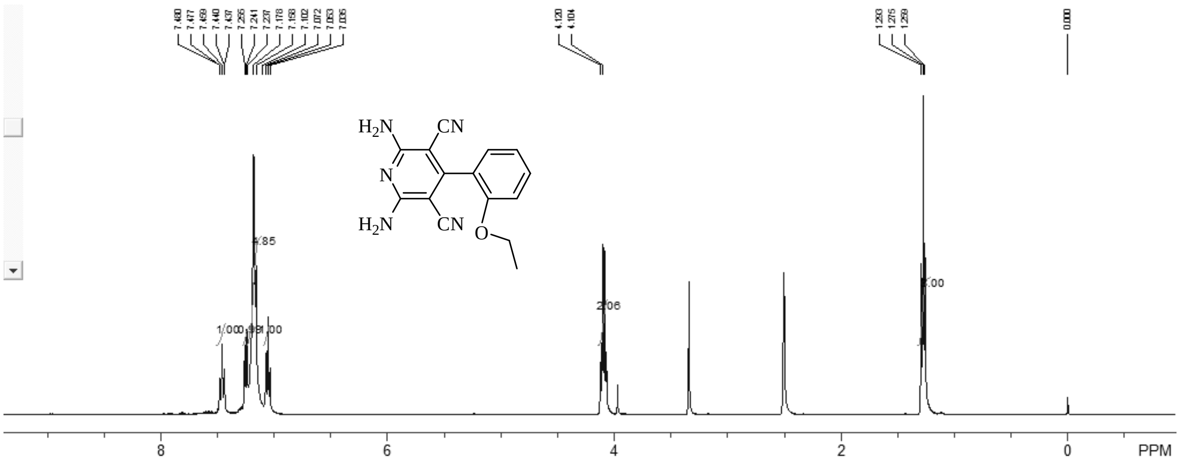

^{13}C NMR spectrum of **6k**

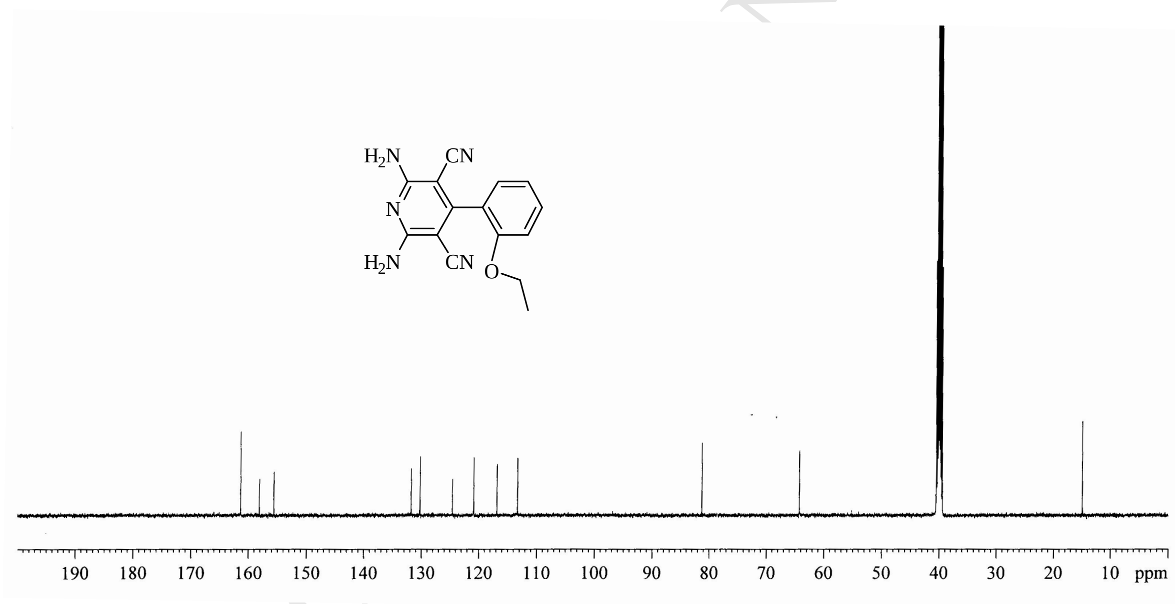

^{1}H NMR spectrum of **6l**

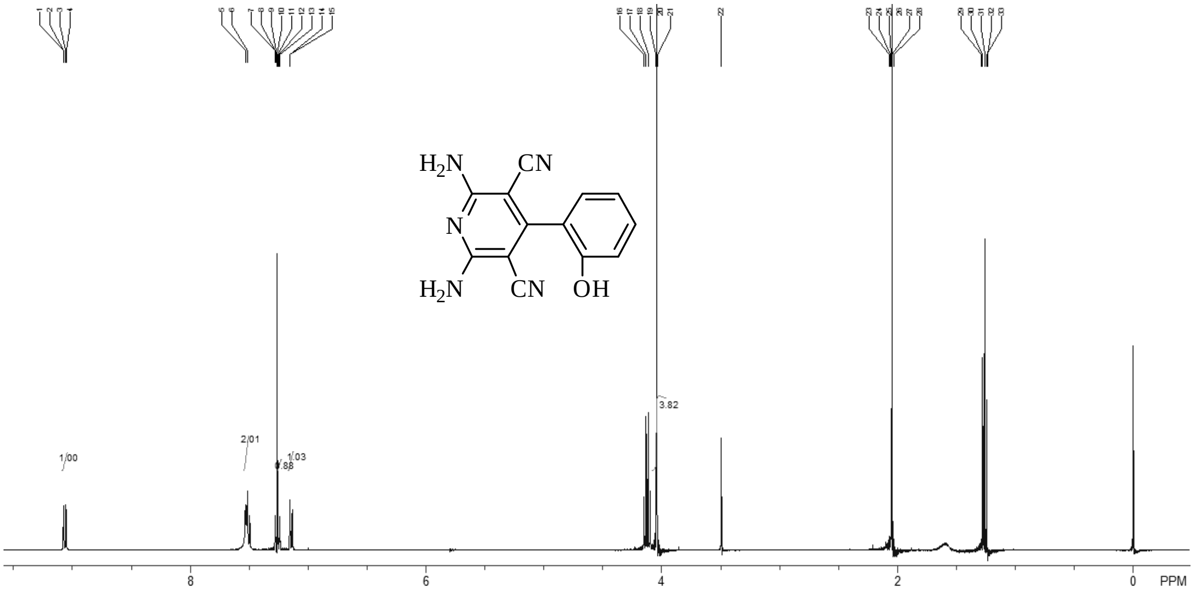

^{13}C NMR spectrum of **6l**

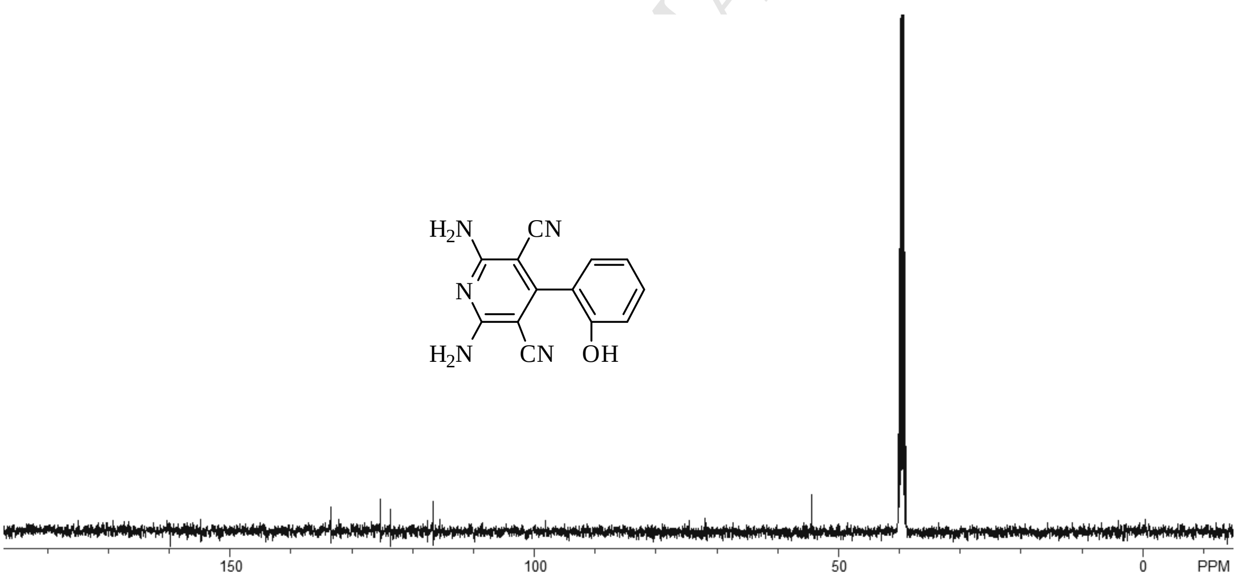

[1]H NMR spectrum of **6m**

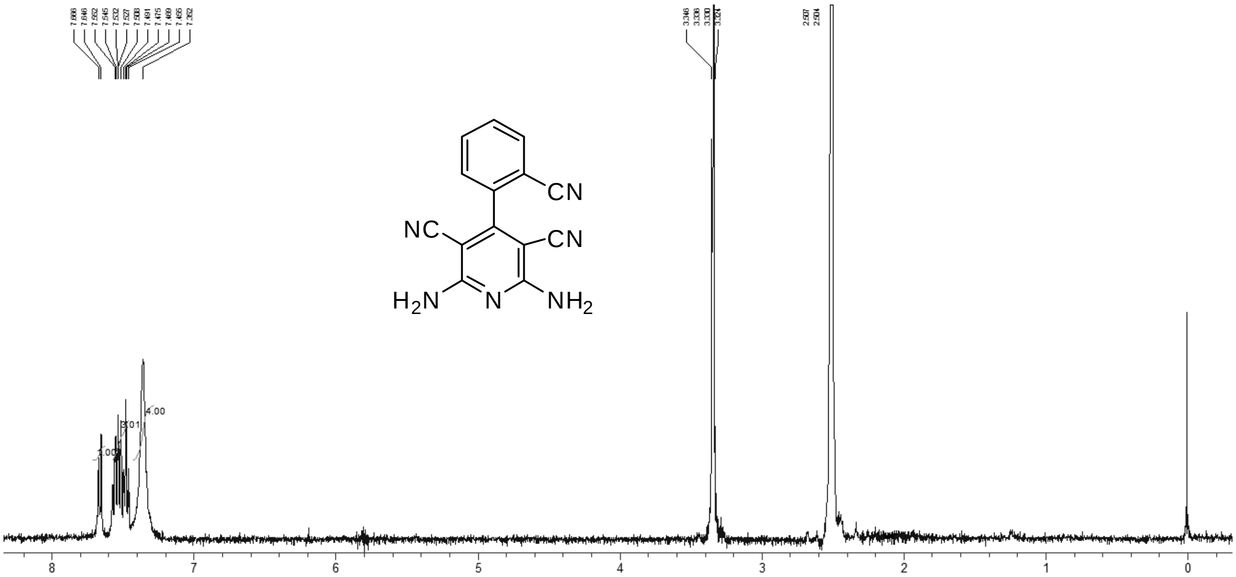

[13]C NMR spectrum of **6m**

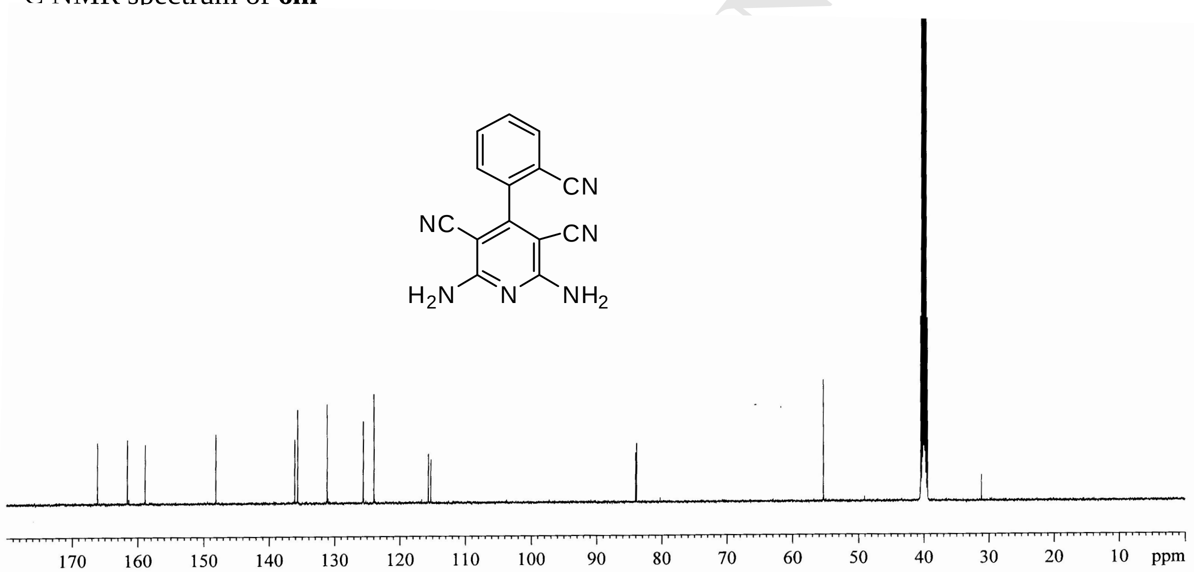

^{1}H NMR spectrum of **6n**

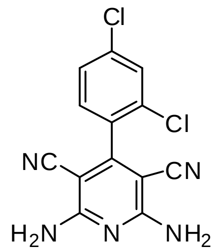

^{13}C NMR spectrum of **6n**

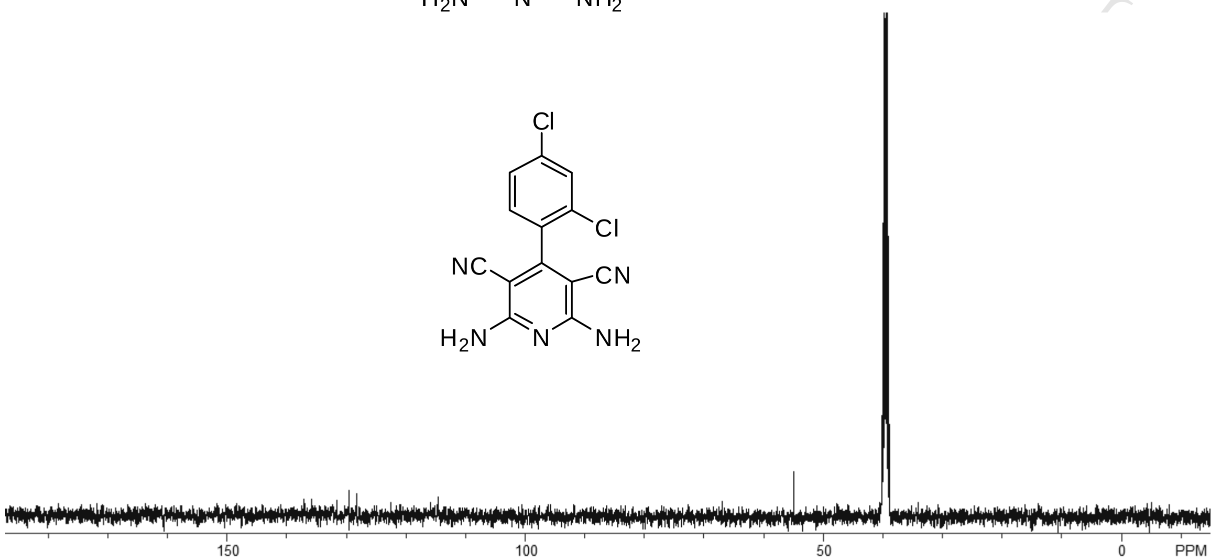

[1]H NMR spectrum of **6o**

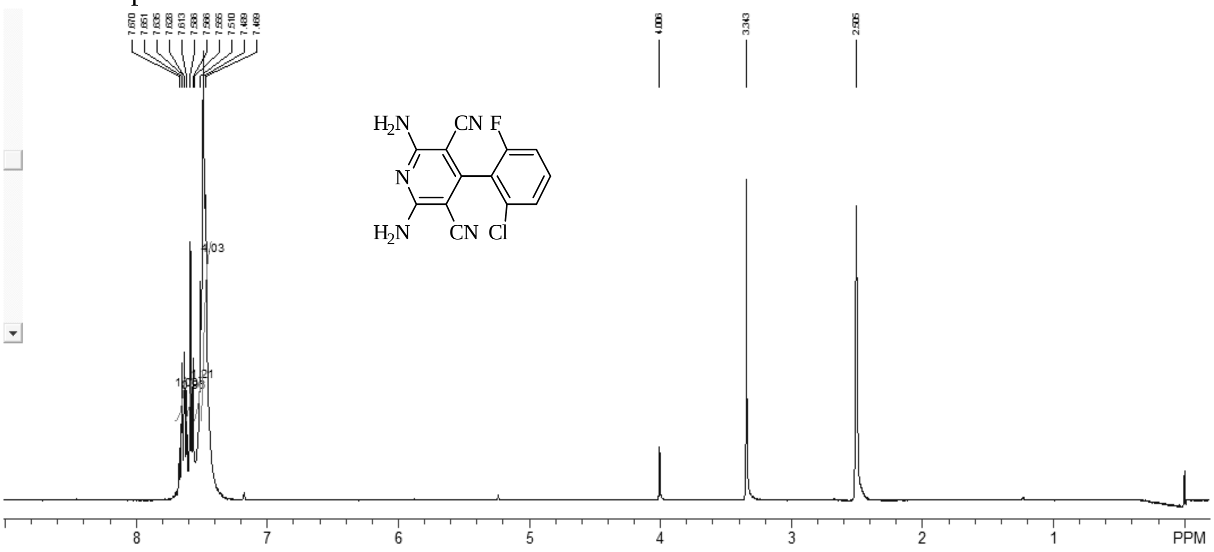

[13]C NMR spectrum of **6o**

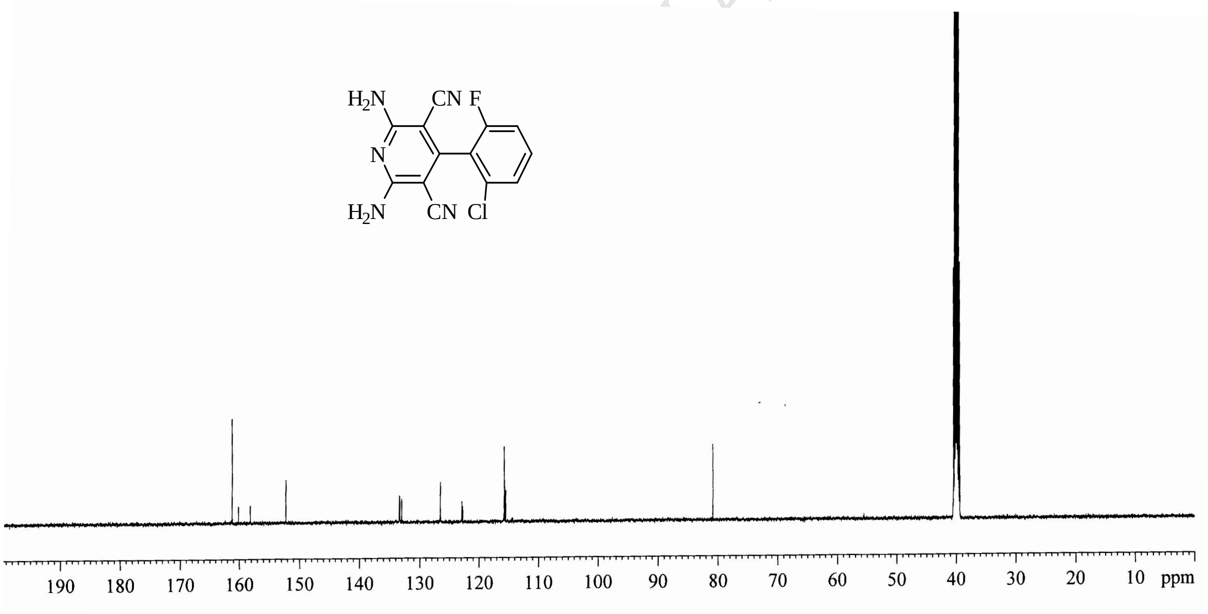

5. Crystal data and structure refinement for 6c

The crystal structure of **6c** was assigned to THF. A summary of the crystal data is given in Table **S1**. with the structure depicted in the main text, where ellipsoids have been drawn at the 50% probability level. Single crystals of **6c** were mounted with glue on glass fiber and crystal data were collected on the Rigaku AFC10 Saturn724 + (2 × 2 bin mode) diffractometer equipped with graphite-monochromated MoKα radiation (λ = 0.710747 Å). Empirical absorption correction was applied using the SADABS program.[S3] The structures were solved by direct methods[S4] and refined by full-matrix least squares on F^2 using the SHELXL-97 program.[S5] All non-hydrogen atoms were refined anisotropically, and the hydrogen atoms were generated geometrically and treated by a mixture of independent and constrained refinement.

Crystallographic data (excluding structure factors) for the structure in this paper have been deposited with the Cambridge Crystallographic Data Centre as supplementary publication no.CCDC 1018482. Copies of the data can be obtained, free of charge, on application to CCDC,12 Union Road, Cambridge CB2 1EZ, UK, (fax: +44 (0)1223 336033 or e-mail: deposit@ccdc.cam.ac.uk).

Table 1

Crystallographic Data and Structure Refinement for compound **6c**

	6
Empirical Formula	$C_{17}H_{11}N_5$· C_4H_8O
Fw	357.41
Temp(K)	153(2)
Wavelength	0.71073 A
Cryst syst	Monoclinic
Space group	P2(1)/n
a (Å)	6.8023(15)
b (Å)	11.459(3)
c (Å)	23.775(5)
□ (deg)	90
□ (deg)	97.832(2)
□ (deg)	90
V (Å^3)	1835.9(7)
Z	4
ρ_c (Mg/m^3)	1.293
Absorption coefficient	0.084 /mm
F(000)	752
Θ range (deg)	3.15 to 28.99

Crystal size	0.50 x 0.19 x 0.17 mm
Limiting indices	-9<=h<=9 -15<=k<=15 -32<=l<=32
No. of reflns collected	19467
No. of indep reflns $R_{(int)}$	4867(0.0336)
Completeness to theta = 28.99	99.7%
Absorption correction	None
Refinement method	Full-matrix least-squares on F^2
data/restraints/params	4867 / 0 / 260
GoF/F^2	1.000
$R1^a$, $wR2^b$(I >2σ(I))	0.0589, 0.1275
$R1^a$, $wR2^b$(all data)	0.0651, 0.1320
Largest diff. peak and hole	0.511 and -0.393 e.A^-3

Table 2

Selected Bond Lengths (Å) and Bond Angles (°)

Bond	Dist.	Bond	Dist.
N(1)-C(5)	1.344(18)	C(2)-C(3)	1.396(18)
N(1)-C(1)	1.345(18)	C(2)-C(6)	1.427(19)
N(2)-C(1)	1.339(18)	C(3)-C(4)	1.394(19)
N(3)-C(5)	1.339(19)	C(3)-C(8)	1.491(18)
N(4)-C(6)	1.149(19)	C(4)-C(5)	1.428(19)
N(5)-C(7)	1.150(2)	C(4)-C(7)	1.429(19)
C(1)-C(2)	1.429(19)		
Angle	**(°)**	**Angle**	**(°)**
C(5)-N(1)-C(1)	119.4(12)	C(2)-C(3)-C(8)	121.5(12)
N(2)-C(1)-N(1)	117.3(13)	C(3)-C(4)-C(5)	119.0(12)
N(2)-C(1)-C(2)	121.0(13)	C(3)-C(4)-C(7)	121.9 (12)
N(1)-C(1)-C(2)	121.7(12)	C(5)-C(4)-C(7)	119.0(12)
C(3)-C(2)-C(6)	120.1(12)	N(3)-C(5)-N(1)	117.6(13)
C(3)-C(2)-C(1)	119.2(12)	N(3)-C(5)-C(4)	120.4(13)
C(6)-C(2)-C(1)	120.7(12)	N(1)-C(5)-C(4)	122.0(13)
C(4)-C(3)-C(2)	118.6(12)	N(4)-C(6)-C(2)	178.8(16)
C(4)-C(3)-C(8)	119.9(12)	N(5)-C(7)-C(4)	176.0(16)

6. REFERENCES

(S1) Sheldrick, G. M. SADABS. Empirical Absorption Correction Program, University of Goettingen, Goettingen, Germany, **1997**.

(S2) Sheldrick, G. M. SHELEX-97, Acta Crystallogr., Sect. A. **1990**; 46: 467-473.

(S3) Sheldrick, G. M. SHELXL-97, Program for Crystal Structures Refinement, University of Goettingen, Goettingen, Germany, **1997**.

checkCIF/PLATON report

You have not supplied any structure factors. As a result the full set of tests cannot be run.

THIS REPORT IS FOR GUIDANCE ONLY. IF USED AS PART OF A REVIEW PROCEDURE FOR PUBLICATION, IT SHOULD NOT REPLACE THE EXPERTISE OF AN EXPERIENCED CRYSTALLOGRAPHIC REFEREE.

No syntax errors found. CIF dictionary Interpreting this report

Datablock: bo2810

```
Bond precision:  C-C = 0.0023 A          Wavelength=0.71073

Cell:            a=6.8023(15)     b=11.459(3)        c=23.775(5)
                 alpha=90         beta=97.832(2)     gamma=90
Temperature:     153 K

                Calculated                 Reported
Volume          1835.9(7)                  1835.9(7)
Space group     P 21/n                     P2(1)/n
Hall group      -P 2yn                     ?
Moiety formula  C17 H11 N5, C4 H8 O        ?
Sum formula     C21 H19 N5 O               C21 H19 N5 O
Mr              357.41                     357.41
Dx,g cm-3       1.293                      1.293
Z               4                          4
Mu (mm-1)       0.084                      0.084
F000            752.0                      752.0
F000'           752.26
h,k,lmax        9,15,32                    9,15,32
Nref            4880                       4867
Tmin,Tmax       0.981,0.986
Tmin'           0.959

Correction method= Not given

Data completeness= 0.997          Theta(max)= 28.990

R(reflections)= 0.0589( 4473)     wR2(reflections)= 0.1320( 4867)

S = 1.000                 Npar= 260
```

The following ALERTS were generated. Each ALERT has the format
test-name_ALERT_alert-type_alert-level.
Click on the hyperlinks for more details of the test.

Alert level G

```
PLAT005_ALERT_5_G No _iucr_refine_instructions_details  in the CIF     Please Do !
PLAT230_ALERT_2_G Hirshfeld Test Diff for    C4     --  C7      ..        5.3 su
PLAT710_ALERT_4_G Delete 1-2-3 or 2-3-4 Linear Torsion Angle ... #         21 Do !
            C3  -C2  -C6  -N4    130.00  7.00   1.555   1.555   1.555   1.555
PLAT710_ALERT_4_G Delete 1-2-3 or 2-3-4 Linear Torsion Angle ... #         22 Do !
            C1  -C2  -C6  -N4    -48.00  7.00   1.555   1.555   1.555   1.555
PLAT710_ALERT_4_G Delete 1-2-3 or 2-3-4 Linear Torsion Angle ... #         23 Do !
            C3  -C4  -C7  -N5     18.00  0.00   1.555   1.555   1.555   1.555
PLAT710_ALERT_4_G Delete 1-2-3 or 2-3-4 Linear Torsion Angle ... #         24 Do !
            C5  -C4  -C7  -N5      2.00  3.00   1.555   1.555   1.555   1.555
PLAT899_ALERT_4_G SHELXL97   is Deprecated and Succeeded by SHELXL       2014 Note
```

---

0 **ALERT level A** = Most likely a serious problem - resolve or explain
0 **ALERT level B** = A potentially serious problem, consider carefully
0 **ALERT level C** = Check. Ensure it is not caused by an omission or oversight
7 **ALERT level G** = General information/check it is not something unexpected

0 ALERT type 1 CIF construction/syntax error, inconsistent or missing data
1 ALERT type 2 Indicator that the structure model may be wrong or deficient
0 ALERT type 3 Indicator that the structure quality may be low
5 ALERT type 4 Improvement, methodology, query or suggestion
1 ALERT type 5 Informative message, check

It is advisable to attempt to resolve as many as possible of the alerts in all categories. Often the minor alerts point to easily fixed oversights, errors and omissions in your CIF or refinement strategy, so attention to these fine details can be worthwhile. In order to resolve some of the more serious problems it may be necessary to carry out additional measurements or structure refinements. However, the purpose of your study may justify the reported deviations and the more serious of these should normally be commented upon in the discussion or experimental section of a paper or in the "special_details" fields of the CIF. checkCIF was carefully designed to identify outliers and unusual parameters, but every test has its limitations and alerts that are not important in a particular case may appear. Conversely, the absence of alerts does not guarantee there are no aspects of the results needing attention. It is up to the individual to critically assess their own results and, if necessary, seek expert advice.

Publication of your CIF in IUCr journals

A basic structural check has been run on your CIF. These basic checks will be run on all CIFs submitted for publication in IUCr journals (*Acta Crystallographica*, *Journal of Applied Crystallography*, *Journal of Synchrotron Radiation*); however, if you intend to submit to *Acta Crystallographica Section C* or *E*, you should make sure that full publication checks are run on the final version of your CIF prior to submission.

Publication of your CIF in other journals

Please refer to the *Notes for Authors* of the relevant journal for any special instructions relating to CIF submission.

PLATON version of 20/08/2014; check.def file version of 18/08/2014

Datablock bo2810 - ellipsoid plot